https://ntrs.nasa.gov/search.jsp?R=19790015339 2020-03-21T23:51:39+00:00Z

9450-46

DOE/JPL 954334-78/9
Distribution Category UC-63

QUARTERLY PROGRESS REPORT

October-December 1978

low cost silicon solar array project

FEASIBILITY OF LOW-COST, HIGH-VOLUME PRODUCTION OF SILANE AND PYROLYSIS OF SILANE TO SEMICONDUCTOR-GRADE SILICON

(NASA-CR-158585) LOW COST SILICON SOLAR ARRAY PROJECT. FEASIBILITY OF LOW-COST, HIGH-VOLUME PRODUCTION OF SILANE AND PYROLYSIS OF SILANE TO SEMICONDUCTOR-GRADE SILICON Quarterly Progress Report, (Union
N79-23510
HC A04/MF A01
Unclas
G3/44 25168

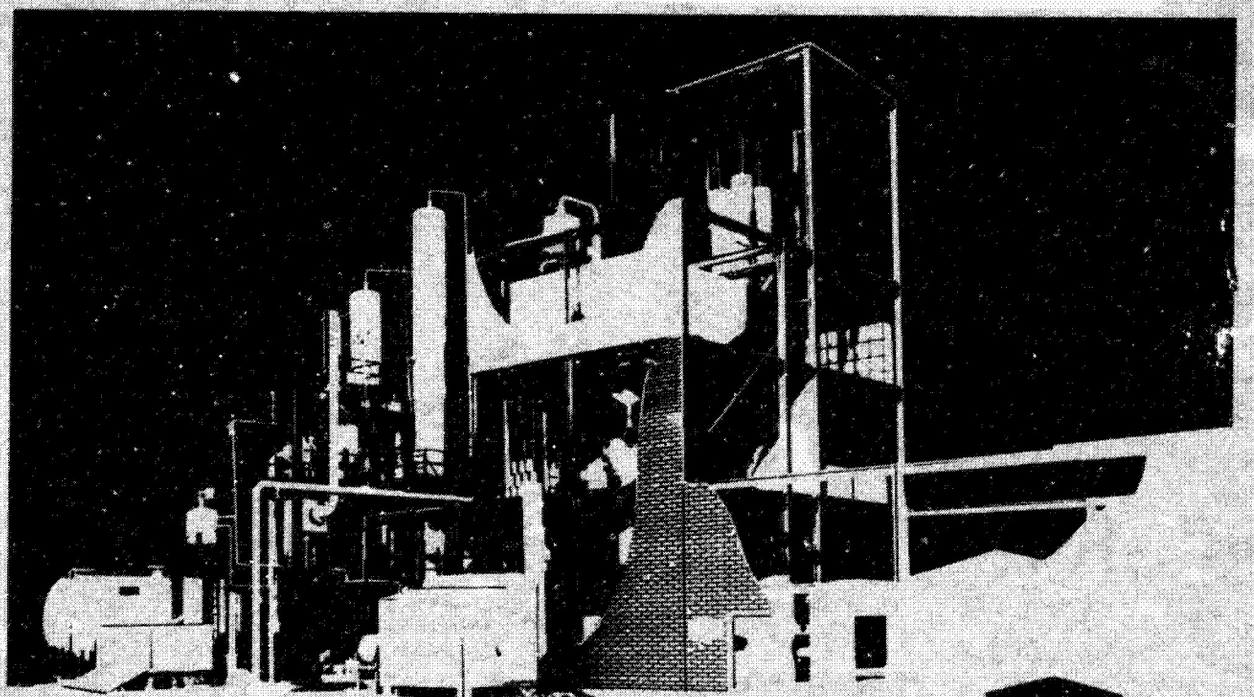

RECEIVED
MAY 1979
NASA ST FACILITY

UNION CARBIDE

UNION CARBIDE CORPORATION

THE JPL LOW-COST SILICON SOLAR ARRAY PROJECT IS SPONSORED BY THE U.S. DEPARTMENT OF ENERGY AND FORMS PART OF THE SOLAR PHOTOVOLTAIC CONVERSION PROGRAM TO INITIATE A MAJOR EFFORT TOWARD THE DEVELOPMENT OF LOW-COST SOLAR ARRAYS. THIS WORK WAS PERFORMED FOR THE JET PROPULSION LABORATORY, CALIFORNIA INSTITUTE OF TECHNOLOGY BY AGREEMENT BETWEEN NASA AND DOE.

DOE/JPL 954334-78/9
Distribution Category UC-63

QUARTERLY PROGRESS REPORT

October-December 1978

low cost silicon solar array project

FEASIBILITY OF LOW-COST, HIGH-VOLUME PRODUCTION OF SILANE AND PYROLYSIS OF SILANE TC SEMICONDUCTOR-GRADE SILICON

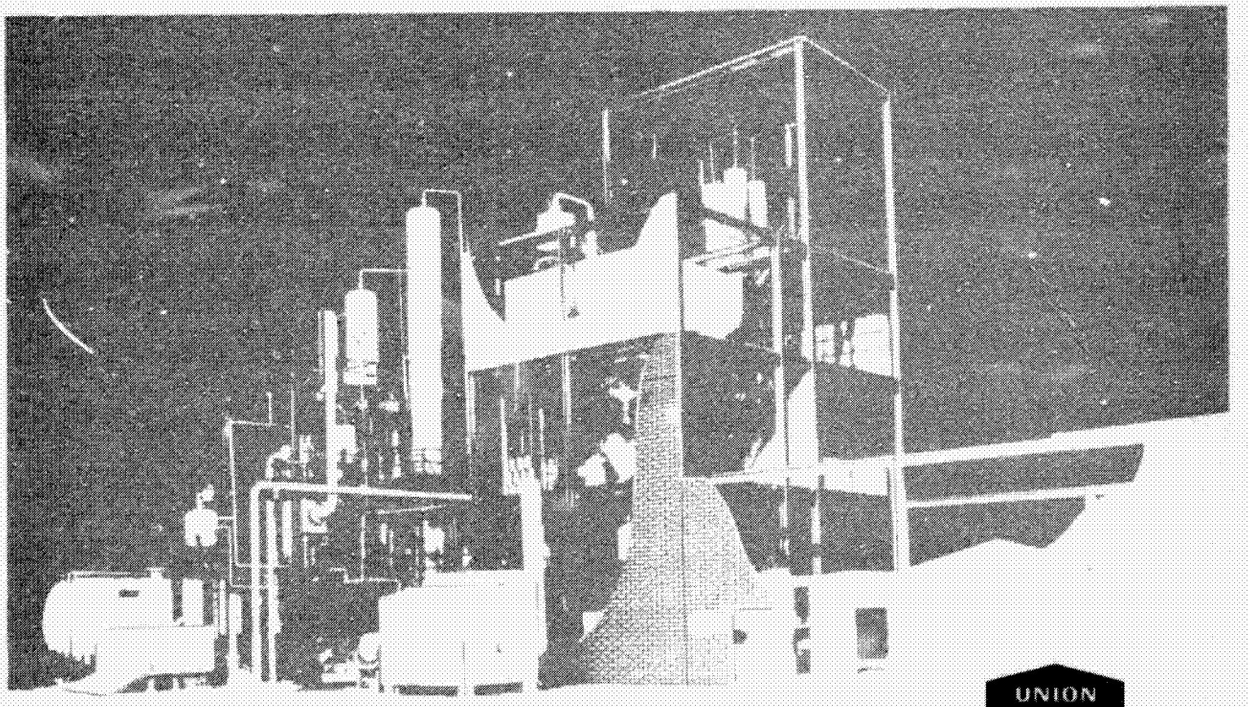

W.C. Breneman E.G. Farrier H. Morihara

UNION CARBIDE CORPORATION

ABSTRACT

SILANE PRODUCTION

The presence of copper promotes a more rapid approach to the steady state operating condition and results in a more consistant reactor effluent composition. The average kinetic and equilibrium yield are unchanged. Incoloy has been identified as the preferred choice of material of construction for the hydrogenation reactor although certain metallurgical changes have been noted in samples exposed to the H_2/HCl atmosphere at $500^{o}C$ which indicate the need for more testing.

SILICON PRODUCTION

The free space reactor and powder storage hopper were operated as a connected unit for nine (9) consecutive silane-to-silicon conversion experiments without opening the reactor. The silicon powder was pneumatically transferred, after each run, to the storage hopper. During the runs, a porous layer of silicon bridged the reactor, but did not impede the silane-to-silicon conversion process. Subsequent design modifications and revised operating procedures effectively prevented powder from accumulating on the reactor lid and on the silane injector. Modifications are presently in progress to prevent the powder from accumulating on the reactor wall.

A new silicon powder melter and feed system was designed and constructed. Dross-free melts were obtained in 152 mm diameter quartz crucibles. In one experiment, 4.4 kg of silicon powder was melted at an average rate of 2.8 kg/hr. The powder feed rate to the melter was programmed and a melting rate as high as 6 kg/hr was maintained for 35 minutes with the powder melting as rapidly as it was fed into the quartz crucible. The powder for the melts was produced in the free space reactor, pneumatically transferred to the storage hopper, and then fed to the melter without exposure to atmospheric contamination.

The compaction behavior of free space reactor powder was evaluated by isostatic pressing and by a manufacturer of briquetting equipment. It was concluded that die pressing and briquetting would result in the production of broken compacts with less than 50% of the theoretical density. Production of sound compacts could be accomplished by isostatic pressing or by the use of additives in die pressing or briquetting.

PROCESS DESIGN

A heat and mass balance of major streams in the Experimental Process System Development Unit (EPSDU), sized for 100 MT/Yr of semiconductor-grade silicon (SGS), was prepared which incorporated most of the process design data obtained in the last quarter. All subsequent process design work discussed in this report is based on this heat and mass balance.

The waste disposal system was completely changed. The chemical oxidation was replaced by thermal oxidation to convert the liquid and gaseous wastes to clean, ventable gas plus liquid and solid bi-products of marketable value instead of landfill.

Equipment specifications were prepared for most of the equipment. They are in sufficient detail to enable vendor quotations and evaluation. A detailed process and instrumentation diagram and an EPSDU layout are under preparation.

A study was conducted to compare the relative merits of suction casting and rapid pulling for polysilicon consolidation. The overall economics on a 1000 MT/Yr scale appear to be roughly the same for these methods, although rapid pulling of poly-rods offers the advantages of less development effort and better quality product samples.

1.2.1 Disproportionation of Chlorosilanes

The kinetics and chemical equilibrium for the liquid phase disproportionation of H_2SiCl_2 and $HSiCl_3$ were studied. The range of experimental conditions bracketed those planned for the larger scale EPSDU facilities. Previous studies of chlorosilane disproportionation reaction parameters used vapor phase reactants and it is important to determine if significant differences would occur with an all liquid system. The catalyst used in this present work was the same type AMBERLYST A-21 tertiary amine functional macroreticular ion exchange resin used earlier.[1] The test apparatus described in detail earlier was operated under sufficient back pressure to assure a 100% liquid chlorosilane stream at the experimental temperature.

The equilibrium conversions using trichlorosilane (H/Cl ratio = 1:3)(Table 1.1) were substantially the same as reported earlier by Bakay[2] for liquid phase reaction. For dichlorosilane feed (H/Cl ratio = 1:1) the equilibrium product mixture showed slightly lower SiH_4 and slightly higher H_3SiCl than that determined by Mui[3] using vapor phase dichlorosilane (Table 1.1) The effect of this variation on the overall process design will be to increase slightly the flow rate through the second disproportionation reactor and require a slightly higher heat duty in the distillation column which separated dichlorosilane from trichlorosilane.

The equilibrium data were obtained in the equipment described earlier[1] by substituting a packed bed reactor 1/4" diameter by 26 foot long for the shorter beds used in the kinetics experiments. This permitted superficial residence times of up to 60 minutes to be obtained at reasonable flow rates.

The liquid phase reaction kinetics for di and trichlorosilane redistribution were studied to provide data for precise design of larger scale reactors. The actual raw data obtained from a series of experiments are listed in Table 1.2.

TABLE 1.1

Equilibrium Compositions
Dichlorosilane and Trichlorosilane
Liquid Phase Redistribution

	32°	56°	81°
SiH_4	11.50 ± .2	11.59 ± .3	11.98
H_3SiCl	15.53 ± .4	16.10 ± .3	16.66
H_2SiCl_2	40.22 ± .4	39.53 ± .4	37.46
$HSiCl_3$	32.62 ± .4	32.69 ± .7	33.36
$SiCl_4$	.13	.10	.54
H/Cl	1.06	1.06	1.06
SiH_4	--	--	--
H_3SiCl		0.38	0.50
H_2SiCl		9.60	9.78
$HSiCl_3$		80.95	80.63
$SiCl_4$		9.08	9.06

Figure 1.1 shows that a close approach to equilibrium is achieved for liquid phase H_2SiCl_2 in about 15 minutes superficial residence time at 56°C where as for vapor phase reactants substantial equilibrium was achieved in about 4 seconds as reported earlier[3]. Thus a vapor phase reactor would convert 2.08 lb. mole of H_2SiCl_2/hr. per cubic foot of reactor volume compared to 2.75 lb. mole/hr for liquid phase H_2SiCl_2.

Figure 1.2 shows that for trichlorosilane, equilibria was achieved in about 40 minutes superficial residence time compared to the 22 minutes reported earlier by Bakay. This variation in reactivity of the resin has been noticed earlier. The process design would incorporate a relatively large reactor bed volume to assure maximum conversion since the catalyst is relatively inexpensive and has a long life.

The small variation in equilibrium composition over the temperature range studied indicates that the overall heat effects are small. The integrated Vaut Hoff equation:

$$\text{In } {}^{K_1}/_{K_2} = - \frac{H}{R} \frac{1}{T_1} - \frac{1}{T_2}$$

applied to the trichlorosilane equilibrium data at 56°C and 81°C gave a heat of reaction of only +2.3 kcal/mole.

An interesting aspect was found during the experimental study which showed bulk diffusional resistance affected the kinetic data at 81°C when the superficial velocities were below 0.75 cm/min. The kinetic data were obtained by varying the reactant flow rate at a fixed bed height. Then different bed heights were used and the profile repeated. Higher conversions were observed at equivalent residence time with increased bed height (higher flow velocities) indicating that bulk film diffusion was becoming the rate controlling feature. The larger scale EPSDU design would utilize flow rates well above the 0.75 cm/min. superficial velocity where film diffusion becomes important.

Figure 1.1

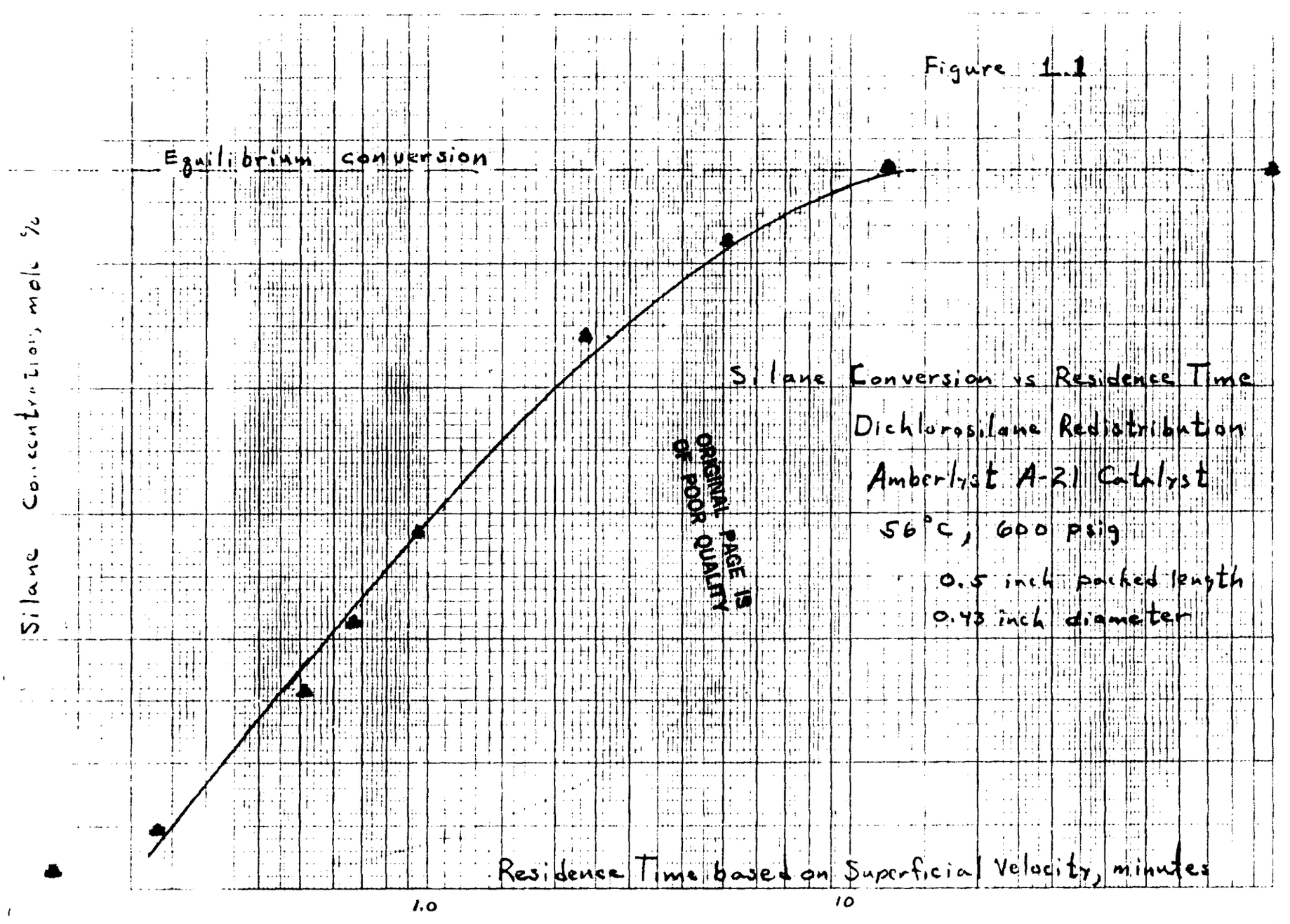
Equilibrium conversion
Silane Concentration, mole %
Silane Conversion vs Residence Time
Dichlorosilane Redistribution
Amberlyst A-21 Catalyst
56°C, 600 psig
0.5 inch packed length
0.43 inch diameter
ORIGINAL PAGE IS OF POOR QUALITY
Residence Time based on Superficial Velocity, minutes
1.0
10

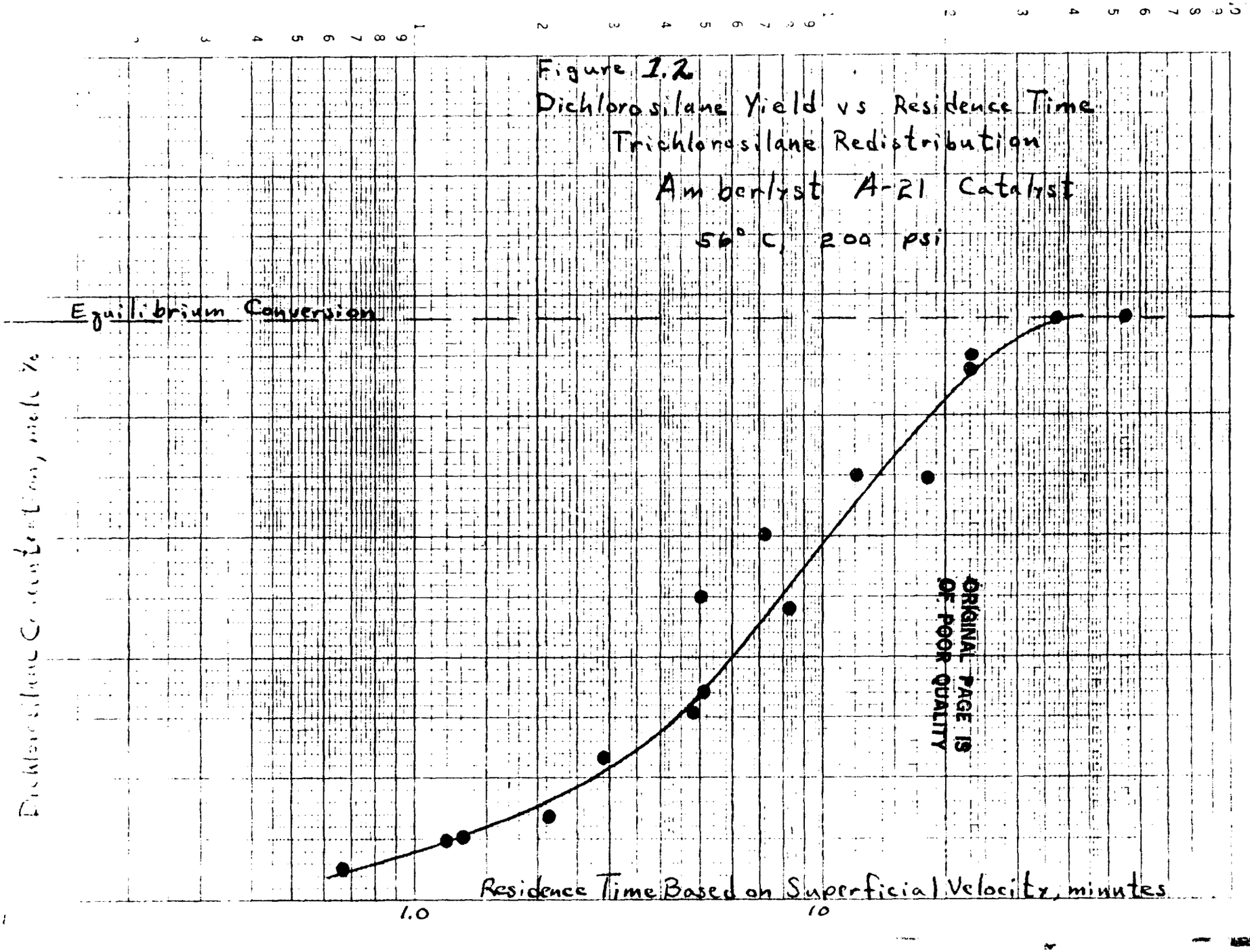
Figure 1.2
Dichlorosilane Yield vs Residence Time
Trichlorosilane Redistribution
Amberlyst A-21 Catalyst
56° C, 200 psi
Equilibrium Conversion
Dichlorosilane Concentration, mole %
Residence Time Based on Superficial Velocity, minutes
1.0
10
ORIGINAL PAGE IS
OF POOR QUALITY

TABLE 1.2

Redistribution of Chlorosilanes
Liquid Phase; Dichlorosilane Feed

T °C	RT Min.	SiH_4 %	H_3SiCl	H_2SiCl_2	$HSiCl_3$	$SiCl_4$	H/Cl Ratio	Bed Height Inches
31	7.17	6.63	17.79	49.43	26.04	0.13	1.045	2.0
31	11.59	7.46	15.35	47.69	29.36		1.01	2.0
31	21.52	8.72	17.02	42.60	31.65		1.03	2.0
31	50.21							2.0
31	0.24	0.25	6.12	89.81	3.57	0.24	1.03	0.5
31	0.54							
31	0.70	0.62	7.81	82.47	9.02	0.09	1.00	0.5
31	0.82	0.66	7.89	82.37	8.99	0.10	1.0	0.5
32	1.00	0.77	8.52	80.31	10.31	0.10	1.0	0.5
32	1.79	1.31	10.52	74.56	13.55	0.10	0.99	0.5
32	5.38	3.11	15.54	56.85	24.44	0.10	0.97	0.5
32	5.38	5.17	14.53	55.75	23.85	0.10	1.01	0.5
32	12.80	6.98	14.89	53.43	24.64	0.06	1,05	0.5
32	60.0	12.85	18.72	37.53	30.85	0.07	1.15	0.5
32	120.0	8.82	16.68	42.72	31.71	0.05	1.02	0.5
32	180.0	6.96	23.24	48.59	21.10	0.1	1.17	0.5
32	1.07	1.21	8.25	80.45	10.04	0.06	1.01	4.0
32	1.92	2.57	10.83	71.27	15.28	0.05	1.01	4.0
32	4.26	6.01	13.22	55.34	25.39	0.04	1.0	4.0
32	6.99	7.48	15.44	49.45	27.63		1.03	4.0
32	14.82	8.03	14.58	42.88	34.51		0.96	4.0
56	0.13	0.28	7.37	85.03	7.12	0.20	1.00	0.5
56	0.23	0.96	11.65	74.98	12.29	0.15	1.01	0.5

TABLE 1.2 (Cont.)

Redistribution of Chlorosilanes
Liquid Phase; Dichlorosilane Feed

T °C	RT Min.	SiH_4 %	H_3SiCl	H_2SiCl_2	$HSiCl_3$	$SiCl_4$	H/Cl Ratio	Bed Height Inches
56	0.51	3.17	13.53	64.85	18.19	0.23	1.01	0.5
56	0.66	4.25	14.58	60.67	20.31	0.20	1.04	0.5
56	0.95	5.69	15.15	55.01	24.02	0.13	1.03	0.5
56	1.70	6.82	16.09	49.20	27.87	0.07	1.02	0.5
56	2.75	8.81	17.18	43.98	29.97	0.08	1.04	0.5
56	5.10	10.38	15.93	42.11	31.41	0.18	1.05	0.5
56	12.13	11.61	16.47	41.15	30.77	0.04	1.10	0.5
56	3.80	9.10	16.34	40.85	33.56	0.07	1.01	2.0
56	2.64	8.84	16.09	44.04	30.98	0.07	1.02	2.0
56	6.80	9.30	16.61	39.89	34.11	0.09	1.01	2.0
56	10.99	9.92	19.36	36.69	33.97	0.07	1.05	2.0
51	20.40	8.15	19.46	36.70	35.69			
56	47.60	3.97	34.73	20.46	40.84		1.02	2.0
56	1.03	5.09	13.91	59.38	21.57	0.043	1.03	4.0
56	1.84	8.31	15.13	47.80	28.73	0.04	1.03	4.0
56	4.25	10.83	16.49	40.72	31.82	0.13	1.06	4.0
56	6.89	10.81	15.80	39.79	33.27	0.24	1.03	4.0
56	27.24	10.96	15.92	39.54	33.22	0.37	1.04	4.0
56	40.70	10.63	16.41	39.43	33.15	0.38	1.04	4.0
31	0.125	1.35	11.34	73.33	13.70	0.29	1.0	0.5
31	0.22	2.93	13.71	64.89	18.26	0.21	1.01	0.5
31	0.50	4.57	20.15	48.23	26.96	0.10	1.02	0.5
31	0.65	6.32	18.72	46.32	28.58	0.09	1.03	0.5

TABLE 1.2 (Cont.)

Redistribution of Chlorosilanes
Liquid Phase; Dichlorosilane Feed

T °C	RT Min.	SiH_4 %	H_3SiCl	H_2SiCl_2	$HSiCl_3$	$SiCl_4$	H/Cl Ratio	Bed Height Inches
81	0.93	6.73	18.56	43.74	30.84	0.13	1.01	0.5
81	1.67	9.38	18.18	40.26	32.44		1.04	0.5
81	1.76	10.62	15.38	39.47	34,31	0.33	1.02	4.0
81	3.90	10.47	16.46	40.06	32.54	0.46	1.04	4.0
81	5.01	8.36	19.48	37.74	34.32			
81	6.53	11.64	16.62	39.05	32.19	0.50	1.07	4.0
81	7.65	7.23	20.90	37.52	34.35			0.50
81	11.93	5.32	24.88	35.43	34.38			0.50
81	16.98	11.61	16.36	38.81	32.74	0.48		4.0

TABLE 1.3

Redistribution of Chlorosilanes

Liquid Phase; Trichlorosilane Feed

T	RT	H_3SiCl	H_2SiCl_2	$HSiCl_3$	$SiCl_4$	Bed Height
56	4.8		4.76	90.64	4.6	
56	4.7		3.10	93.87	3.03	0.5
56	4.7		3.03	94.19	2.78	
56	2.0		1.97	96.42	1.61	
56	2.0		1.75	96.74	1.51	
56	1.3		1.26	97.72	1.02	
56	1.3		1.04	98.04	0.92	
56	2.1		1.38	97.29	1.33	
56	2.1		1.37	97.40	1.23	
56	1.2		0.99	98.13	0.88	
56	1.2		0.97	98.16	0.87	
56	0.63	0.15	0.57	98.79	0.49	
56	0.63	0.11	0.51	98.92	0.46	
81	2.1	0.07	3.89	92.65	3.39	
81	2.1	0.08	3.96	92.52	3.49	
81	1.0	0.03	2.43	95.41	2.13	
81	1.0	0.02	2.44	95.44	2.10	
81	0.61		1.77	96.83	1.40	
81	0.61		1.69	96.85	1.46	

Table 1.3 (Cont.)

$HSiCl_3$ Redistribution

2" Bed Height

P=200 psi

T °C	RT Min.	SiH_4	H_3SiCl	H_2SiCl_2	$HSiCl_3$	$SiCl_4$	Bed Height
56	18.5		0.13	7.03	86.37	6.47	2.0
56	18.5		0.12	6.88	86.57	6.43	
56	8.2	0.04	0.05	4.60	91.23	4.08	
56	8.2	0.06	0.06	4.81	90.91	4.16	
56	5.1	0.16	0.02	3.46	93.32	3.04	
56	5.1	0.04	0.03	3.45	93.53	2.95	
56	5.1			3.38	93.79	2.83	
56	2.8		0.03	2.38	95.62	1.97	
56	2.8		0.03	2.32	95.58	2.04	
81	9.3		0.69	9.42	80.70	9.19	
81	9.3	0.53	0.44	9.53	80.86	8.64	
81	4.1	0.03	0.19	7.38	85.81	6.59	
81	4.1		0.22	7.33	85.86	6.59	
81	2.2	0.21	0.35	5.89	88.58	4.97	

Table 1.3 (Cont.)
$HSiCl_3$ Redistribution Data

T	RT Min.	H_3SiCl	H_2SiCl_2	$HSiCl_3$	$SiCl_4$	Bed Height
55.5	7.2	0.14	6.25	88.62	4.99	4.0
55.5	7.2	0.18	5.93	88.33	5.56	
56.0	12.22	0.22	7.08	86.08	6.62	
56.0	12.2	0.21	7.18	86.05	6.56	
56.0	5.1	0.18	5.01	90.32	4.49	
56.0	5.1	0.15	5.02	90.16	4.67	
56.0	23.5	0.25	8.75	82.65	8.34	
56.0	23.5	0.23	8.90	82.76	8.11	
56.0	23.5	0.22	9.39	82.34	8.05	
56.0	36.55	0.43	9.17	81.82	8.58	
56.0	36.55	0.34	9.60	81.37	8.69	
56.0	36.55	0.25	9.56	81.37	8.82	
56.0	52.7	0.36	9.58	81.07	8.99	
56.0	52.7	0.40	9.62	80.82	9.16	
81.0	7.9	0.37	9.81	80.11	9.71	
81.0	7.9	0.46	10.16	79.40	9.98	
81.0	5.0	0.34	9.06	81.27	9.33	
81.0	5.0	0.48	8.99	81.58	8.95	
81.0	14.45	0.46	10.64	78.72	10.18	
81.0	14.95	0.45	10.66	78.77	10.12	
81.0	27.2	0.50	10.63	78.66	10.21	
81.0	27.2	0.57	10.72	78.55	10.16	
180		0.66	9.79	80.52	9.03	
180		0.33	9.77	80.74	9.16	

1.2.2 Hydrogenation Studies

A study of the effects of various loadings of copper catalyst on the kinetics of hydrogenation of $SiCl_4$ in the presence of metallurgical grade silicon showed that very little or no copper may be required to achieve modest reaction rates. The studies were made at 500°C and 50 psig in the 1" diameter high pressure fluid bed reactor described earlier[6]. The effect of copper loading was studied at levels of 0, 1, and 2%. the copper/silicon blend was prepared by simple mixing of cement copper[1] with metallurgical silicon. The individual experiments were carried out for 9 - 15 hours in each case to assure that steady state conditions were in effect and to remove any transient copper/silicon interactions which occur during the initial reaction period. As shown in Figure 1.3, the conversion at 6.4 seconds superficial residence time was 15.7 $\pm$ 1.6% for 0% copper and 14.8 $\pm$ 0.8% for 0.63% copper retained by the silicon/copper mass. The retention of copper by the mass was 32 - 38% as determined by atomic adsorption analysis of the reactor contents at the end of the run. The amount of copper / silicon alloy was 0.37% when 2% copper was originally charged and only 0.03% when 1% copper was initially used. The constancy of the reactor yield was noticeably improved and the time required to reach the average performance level was reduced when copper was used. However, the overall yield after achieving steady state operation was not significantly altered. At the temperature, pressure and stoichiometry used, the equilibrium conversion is 20.5%. Previous experiments by Mui[5] using 2.0% copper added as a cement copper indicated 15.3% $HSiCl_3$ at 6.4 seconds residence time by extrapolation. The lower reaction rate when 1% copper was used and the variable conversion at 0% copper indicates that the reaction mechanism is also influenced by other properties of the silicon. Previous electron micrographs (SEM) of metallurgical silicon containing copper catalyst indicated that attack on the silicon occurred only at sites occupied by copper - but that not all sites occupied by copper were attacked. Scanning electron

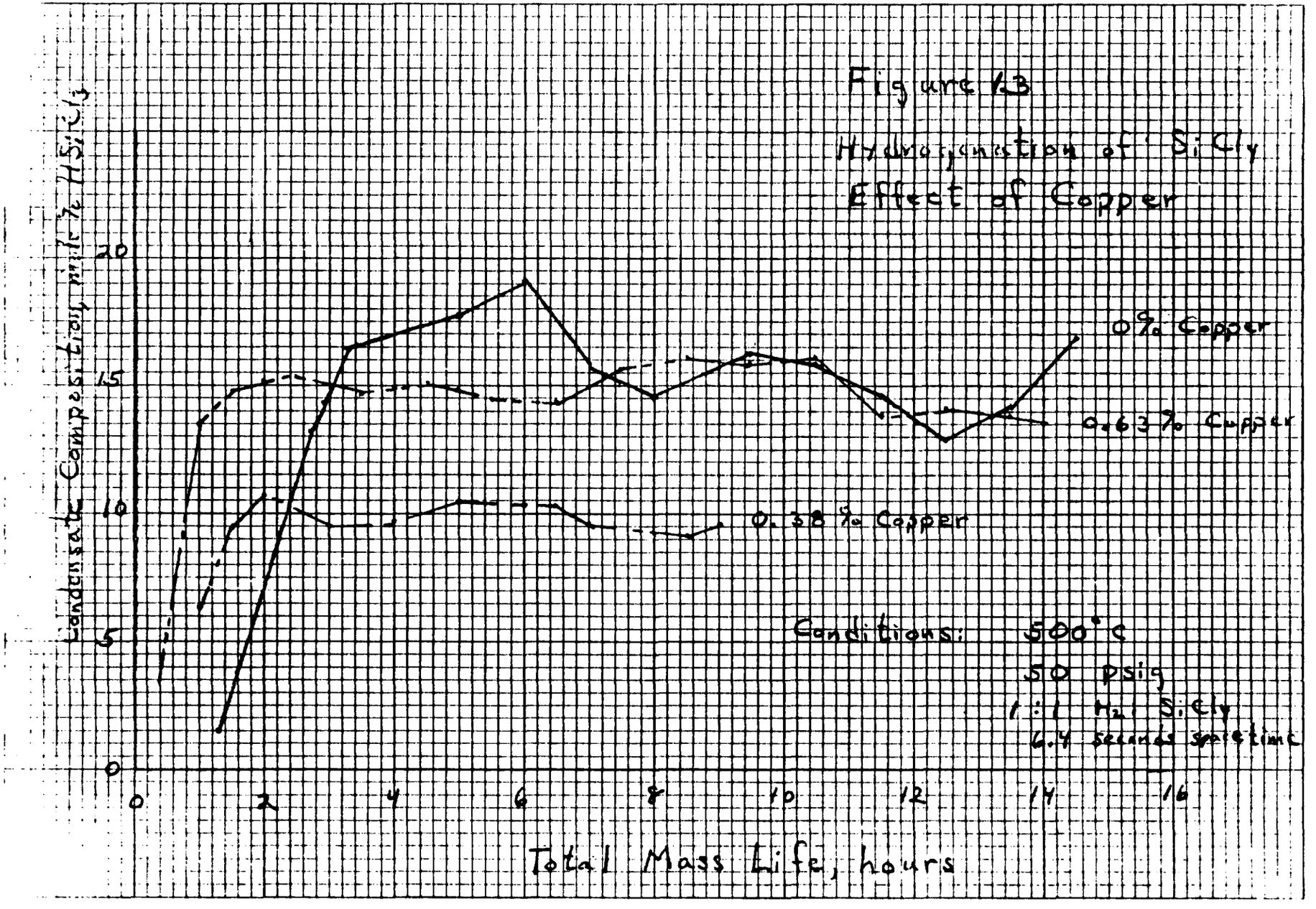
Figure 43
Hydrogenation of SiCl4
Effect of Copper
Condensate Composition, mole % HSiCl3
Total Mass Life, hours
0% Copper
0.63% Copper
0.38% Copper
Conditions:
500° C
50 psig
1:1 H2 : SiCl4
6.4 seconds space time
0
5
10
15
20
0
2
4
6
8
10
12
14
16

micrographs (SEM) of metallurgical silicon exposed to the reaction conditions in the presence of various levels of copper give insight into the reaction mechanism. Figure 1, a-d shows particles of metallurgical silicon (100 x 250 micron). The unreacted, copper free silicon (a) has smooth surface features, sharp edges and no dust particles. After 10% conversion of the silicon by reaction of H_2 and $SiCl_2$ at 500°C, 50 psi, photo (b) shows etching is occurring at specific reaction sights - primarily starting at the edges and then spreading into and over the particle. Little attack occurred on the smooth surfaces of the particle. Again, no fine particles were seen at this low conversion.

In (c) and (d) copper in the form of a mixture of oxides and metallic copper with an average particle size of 10 microns was blended with the silicon charge to the reactor. After an equivalent exposure to the reaction conditions producing essentially the same yield of trichlorosilane the amount of etching appears to be significantly increased. Etching now occurs more generally over the surface of the silicon and many fine particles are also seen which do not appear to originate from the silicon and are of a size equivalent to the 10 micron cement copper.

The "cement copper", a mixture of oxides has been shown to reduce quickly with H_2 at 500°C:

$$CuO + H_2 \longrightarrow Cu + H_2O \quad (1)$$

$$Cu_2O + H_2 \longrightarrow 2Cu + H_2O \quad (2)$$

The water produced reacts with the silicon tetrachloride and can etch silicon by the sequence:

$$2H_2O + SiCl_4 \longrightarrow SiO_2 + 4HCl \quad (3)$$

$$4HCl + Si \longrightarrow SiCl_4\ (+HSiCl_3) + 2H_2 \quad (4)$$

A predominant feature in (d) is the presence of small light tone particles in the craters of the etched silicon. This implies that some activating phenomena is occurring locally and resulting in faster etching. However many areas of the silicon also show these small particles without cratering. Again, the entry point for attack seems to be the sharp edges of the silicon particles and to a much lesser extent on the planar surfaces. Thus it could be that two rather independent actions are occurring, the etching of silicon at sites active because of crystal defects and copper reduction with concurrent HCl etching of silicon in the proximity of the copper reduction. There is still no clear evidence that copper is necessary to promote the hydrogenation reaction other than to cause increased locallized etching of silicon immediately after reactor start up.

It has been shown earlier that $CuCl_2$ can also be formed in this system from a reaction:

$$Cu + 2HCl \rightarrow CuCl_2 + H_2 \qquad (5)$$

the $CuCl_2$ can react with silicon metal to form a copper/silicon alloy:

$$6CuCl_2 + 5Si \rightarrow 2Cu_3Si + 3SiCl_4 \qquad (6)$$

Thus in a fairly complex but thermodynamically favored scheme, silicon can be etched by copper oxide in the presence of H_2 and $SiCl_4$ and the resulting silicon surface could be made locally more sensitive to further attack in a fashion which would regenerate Cu_3Si. Thus the mere presence of CuO in the system should result in more etching of the surface due to the reaction sequences :

$$1 \text{ or } 2 \longrightarrow 3 \longrightarrow 4 \quad \text{and}$$
$$3 \longrightarrow 5 \longrightarrow 6$$

The first sequence would also tend to show the formation of particles of white silica in the reaction mass. Every two atoms of oxygen in the cement copper would result in an atom

FIGURE 1.4

SCANNING ELECTRON MICROGRAPHS OF Cu/Si CONTACT MASS

180 x

ORIGINAL PAGE IS
OF POOR QUALITY

of Si being rapidly etched by the first scheme and 6 atoms of O resulting in 5 atoms of etched Si by the second scheme. The level of alloy in the 2% copper experiments was measured at 0.37% or about 20% of the charged copper.

1.2.3 Materials of Construction

Carbon steel has been identified as the material of choice for the packed bed catalystic disproportionation reactors based on analysis of test coupons from the Process Development Unit, PDU, reactors. Prior to the initial operation of the PDU, a set of test coupons of 316 stainless steel and carbon steel were placed inside the packed bed reactor in contact with the resin and liquid chlorosilane stream. These coupons were removed after 6,000 hours of exposure to the process environment (25^{o} - 60^{o}C) and examined. By weight loss it was determined that the corrosion rates were:

Carbon Steel	0.0003 inches/year
316 Stainless Steel	0.0007 inches/year

Low power microscopic examination showed evidence of pitting attack on the 316 SS at the crevice formed by the mounting hardware (also 316 SS) and the coupon.

From many years experience with processing high purity chlorosilanes it has been found that carbon steel does not contribute impurities to the process stream providing the system is maintained in a bone dry state and that "new"piping is first conditioned to the chlorosilane environment. These three factors indicate that carbon steel would be the material of choice for these reactors.

The processing environment of the hydrogenation reactor has resulted in significant attack on all metals tested to date. The best material identified so far is Incoloy (Table 1.4).

Table 1.4

Corrosion Test Results

Hydrogenation Reactor

Material	Penetration Inches/Year*
316 Stainless Steel	0.8240
Inconel 825	0.4113
Incoloy	0.1578
Chrome Plated Steel	1.5713
26-1 Steel	0.9148
Titanium	Reactive - Coupon Consumed

* Based on 36 hours actual to reaction temperature, 500°C $H_2/SiCl_4$ atmosphere and Cu/Si Mass.

The combination of temperature (500°C) and hydrogen and hydrogen chloride partial pressure presents an environment extremely hostile to many metal alloys. Figure 1.5, a-c shows the nature of the attack on Inconel 600. The thermocouples shown here have a loosely adhering scale rich in silicon after relatively short exposure at 500°C. The thickness of the Inconel is about 0.02 inches. The one shown in Figure 1.5b was exposed for one hour at 900°C after previous exposure for 36 hours at 500°C. The sheath has been penetrated and the functional use lost. Exposure of about 100 hours of one Inconel sheathed thermocouple resulted in light surface pitting under the scale deposits. However, the normally non-magnetic austenitic structure had been replaced by a ferritic type magnetic character. The same result occurred with a 304 stainless steel sheath but in a shorter time.

Figure 1.5 d shows the condition of other materials after 36 hours exposure after the surface scale had been brushed off. The Incoloy has the best appearance and the lowest weight loss. The chrome plate carbon steel, although showing the largest weight loss showed very little attack where the chrome plating was still intact.

Although Incoloy is the best candidate to-date, testing continues using high chrome alloy following the lead of the chrome plated steel.

1.2.4 Silane Vapor Liquid Equilibrium Studies

Development of a chromatographic method for separating phosphine, silane, argon and diborane was initiated this period. In conjunction with a vapor-liquid equilibrium cell immersed in a cryostat the analytical method will be used to determine the Henry's Law constant for these compounds.

It was determined that a cross-linked polystyrene type column packing, Chromasorb 104 was suitable for separating a silane-phosphine mixture. A 1/8" diameter, 6 foot long column at 50°C oven temperature resulted in a phosphine retention time of 2.4 minutes. The sensitivity was measured at 0.0351 millimoles per unit area on the Lab Pace computer aided chromatograph used.

The initial trials using a diborane/argon mixture were unsuccessful at achieving an identifiable peak for diborane using either Chromasorb 104 or OV 101/Chromasorb WHP a column routinely used to separate silane from chlorosilanes.

1.3 CONCLUSIONS

- The kinetics and equilibrium product composition for the liquid phase disproportionation of dichlorosilane and trichlorosilane are compatible with and reinforce the reliability of the latest EPSDU process design.

- Carbon steel is preferred over 316 stainless steel as a material of construction for the disproportionation packed bed reactors because of less crevice corrosion.

- Incoloy, the preferred choice of material for the hydrogenation reactor, is subject to modest attack by the H_2/HCl atmosphere at 500°C.

1.4 PROJECTED QUARTERLY ACTIVITIES

- Study silane/diborane, phosphine vapor liquid equilibrium.

- Continue studies of effect of copper on hydrogenation reaction at higher pressures.

1.5 REFERENCES

1. Breneman, W. C., Farrier, E. G., Morihara, H., Low Cost Silicon Solar Array Project Quarterly Report DOE/JPL 954334-78/B

2. Bakay, C. J., U. S. Pat. 3,928,542

3. Breneman, W. C., Mui, J. Y. P., Low Cost Silicon Solar Array Project Quarterly Report DOE/JPL 954334-76/3

4. Friedel, Ladenburg, Bull. Soc. Chem. (2) 12, 92-7 (1869)

5. Breneman, W. C., Mui, J. Y. P., Low Cost Silicon Solar Array Project Quarterly Report DOE/JPL 954334-78/6

6. Ibid 77/4

2.1 INTRODUCTION

The objective of this program, which started in January, 1977, is to establish the feasibility and cost of manufacturing semiconductor grade polycrystalline silicon through the pyrolysis of silane (SiH_4). The silane-to-silicon conversion is to be investigated in a fluid bed reactor and in a free space reactor.

In the third quarter of 1978, it was reported that the fluid bed reactor was operated continuously for 48 hours with a mixture of one percent silane in helium as the fluidizing gas. A high silane pyrolysis efficiency was obtained without the generation of excessive fines. Dense, coherent plating was obtained on the silicon seed particles which had remained fluidized throughout the experiment. During the current quarter, no additional fluid bed reactor experiments were performed, and a rough draft of a report was completed summarizing the fluid bed reactor program.

In the third quarter of 1978, it was also reported that the free space reactor was operated for eight (8) consecutive silane pyrolysis experiments, and that methods were investigated for converting the free space reactor powder into a more suitable feedstock for silicon melters. Among the methods investigated were loose powder sintering, conventional die pressing, and direct rolling of flakes.

2.2 DISCUSSION

The ninth consecutive silane pyrolysis experiment was completed in the free space reactor during this quarter.

In these experiments, silane was pyrolyzed to form silicon powder for a total of 38 1/2 hours without opening or servicing the reactor. Approximately 19 kg of silicon powder were produced at an average production rate of 0.50 kg/hr. After each pyrolysis experiment, the silicon powder was pneumatically transferred from the settling chamber (located beneath the reactor) to a storage hopper.

2.2.1 FREE SPACE REACTOR

Inspection of the free space reactor after 38 1/2 hours of production revealed that the quartz liner was cracked and a porous layer of silicon had bridged the reactor. Six large fragments of the porous silicon were in the settling chamber. The bridged section adhering to the quartz was approximately 140 mm thick. Above the bridge, the reactor and injector were covered with a 6 mm thick layer of silicon powder. Beneath the bridge, the silicon wall coating varied in thickness from 13 mm near the bridge to 25 mm near the base of the reactor. It was hypothesized, by comparing the amount of powder pneumatically transferred with the calculated amount produced, that the bridge and fragments formed gradually during the nine (9) consecutive runs. It was not known when the wall formations finally bridged the reactor because none of the process sensors (thermocouples, pressure gauges, flow meters, etc.) indicated that the reactor performance during the last run was any different than that of previous runs in this series of experiments. The top of the bridge was fairly level and powdery, while the bottom was irregular and contained a 50 mm diameter x 130 mm long cone-shaped section. The injector tip, although not attached to the semi-solid silicon of the bridge, was submerged in powder. Since the silicon bridge was porous and the lower cone-shaped formation contained

channels, the bridge could have acted as an extension of the injector. This extension would have placed the point of silane injection into the hotter regions of the reactor where conditions were more favorable for the formation of injector cones. During the remainder of this quarter, free space reactor experiments were conducted to provide silicon powder for a new melter, to identify the conditions which initiated the formation of the porous bridge, and to establish reactor operating conditions and/or reactor design modifications which minimize or prevent powder from adhering at critical locations.

In an effort to identify the conditions that initiate the formations that eventually bridge the free space reactor, silane-to-silicon conversion experiments were conducted for 2-, 4-, 6-, and 8-hour durations under similar operating conditions. After each experiment, the reactor lid was gently removed after the reactor had cooled to room temperature. The cooling process, or breaking the lid seal, typically caused the powder adhering to the lid, the gas injector and on the reactor wall near the flange to fall into the reactor. After most of the experiments, the powder did fall as the lid was removed from the reactor. This made it difficult to formulate a model depicting the mechanism of formation of the porous bridge. However, the following observations were made: powder buildup starts at the corners where the injector meets the lid and where the lid meets the reactor. After four hours of silicon production, powder adhering to the reactor wall for a distance of 80 to 90 mm above and below the tip of the injector was approximately 1 mm thick. After six hours of production, a 70 to 100 mm thick deposit was momentarily seen on the injector. This powder fell into the reactor leaving the injector and lid

relatively free of powder. The reactor wall in the vicinity of the injector tip retained a 50 mm thick powder deposit. All of the powder deposits felt loose and fluffy, except for the deposit that remained adjacent to the quartz liner after the loose powder was removed. The deposit adhering to the quartz liner was dark gray and gritty. After the eight-hour run, the reactor was completely bridged over with a porous mixture of silicon powder, agglomerated friable clusters, and shiny, silver metallic deposits. A 100 mm diameter powder deposit was seen momentarily on the injector, and the deposit on the lid was estimated to be 20 mm thick. The results of these experiments seem to indicate that bridging can be prevented if: 1) reactor operating conditions are established which minimize the powder buildup on the water-cooled injector and in the recirculation region above the injector tip, and 2) the reactor design modifications prevent the powder from building-up in the critical regions.

Experiments were conducted to establish reactor operating conditions and/or reactor design modifications that minimize or prevent powder from adhering to the reactor at critical locations. Varying the reactor operating temperature between 680° C and 720° C did not significantly reduce powder buildup on the reactor wall near the silane injector nor on the reactor lid or the water-cooled injector. A reactor lid containing a porous metal sheet, through which a gas could be fed into the reactor, was designed, constructed, and tested. A mechanical powder stripper which surrounded the injector was also installed in the reactor lid. Examination of the reactor after the runs were completed revealed that the procedure of pulsing argon through the porous plate dislodged any powder which might have accumulated on the lid of the reactor. The powder deposits on the injector were

also controlled. Although the reactor wall appeared free of adhering powder after some experiments, these results were not consistently obtained. When powder deposits were observed on the reactor wall near the injector tip, the wall deposits varied from 10 to 50 mm thick for separate eight-hour duration experiments. Consequently, a device was designed for mechanically removing the wall deposits intermittently during the course of the silane pyrolysis experiments. This device will be constructed and its behavior evaluated next quarter.

2.2.2 SILICON POWDER TRANSFER

The current powder storage hopper has a capacity of approximately 100 ℓ. The powder conveying components of the hopper were redesigned to afford a more reliable and controllable feed rate for powders of varying densities. A porous metal filter (35 μm average pore size) was installed as an integral part of the hopper lid for gas-powder separation during pneumatic powder transfer from the settling chamber. A fluid slide located in the conically shaped lower portion of the hopper aided in gravity feeding the powder to the bottom of the hopper. A vertical auger inside the hopper, with an attached sweep arm, controlled the rate of powder discharge from the hopper. With the above system, controllable powder discharges were obtained.

2.2.3 SILICON CONSOLIDATION

2.2.3a SILICON POWDER MELTING

A new silicon powder melter and feed system were constructed. Figure 1 is a photograph showing the furnace, quartz feed tube, and the 100 ℓ capacity

storage hopper. Figure 2 is a view of the inside of the melter, again showing the quartz feed tube. Figure 3 is a schematic (not to scale) of the melter. During the melting operation, silicon powder is transferred from the storage hopper through the quartz tube (which has a 10° C downward pitch) by means of the enclosed auger. The powder is dropped through the vertical section of the quartz tube into the quartz crucible (152 mm diameter x 178 mm high). The end of the quartz tube projects slightly below the rim of the crucible.

To date, eight melting experiments were conducted during the performance evaluation tests. In the last three experiments, dross-free castings were obtained. In the last melting experiment, approximately 4.4 kg of silicon powder from the free space reactor was melted. The powder feed and melting rate were programmed. The powdered silicon was slowly fed into the hot (1600° C) crucible until a molten puddle of silicon was obtained. Initially, heat was supplied by an inductively-heated graphite susceptor which surrounded and supported the quartz crucible. Once the molten puddle of silicon was obtained, the silicon appeared to suscept and the power required to maintain 1600° C decreased from approximately 17 kw to 14 kw. As the surface area of the molten silicon increased, the powder feed rate was increased. From data previously obtained on the powder discharge rate from the storage hopper, it was estimated that a melting rate of 6 kg/hr was obtained. This powder feed rate was maintained for 35 minutes with the powder melting as rapidly as it was fed into the quartz crucible. For the 4.4 kg melt, an average melting rate of 2.8 kg/hr was obtained. This experiment completes the task of testing the reliability of the new melter. Additional melting experiments will be performed in conjunction with a five (5) consecutive run demonstration.

ORIGINAL PAGE IS
OF POOR QUALITY

Figure 1. Melter and storage hopper assembly.

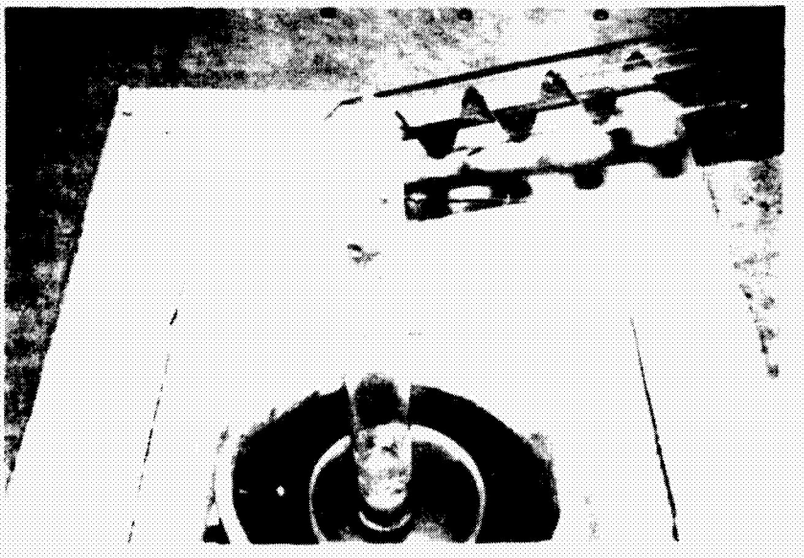

Figure 2. Quartz feed tube for melter with auger.

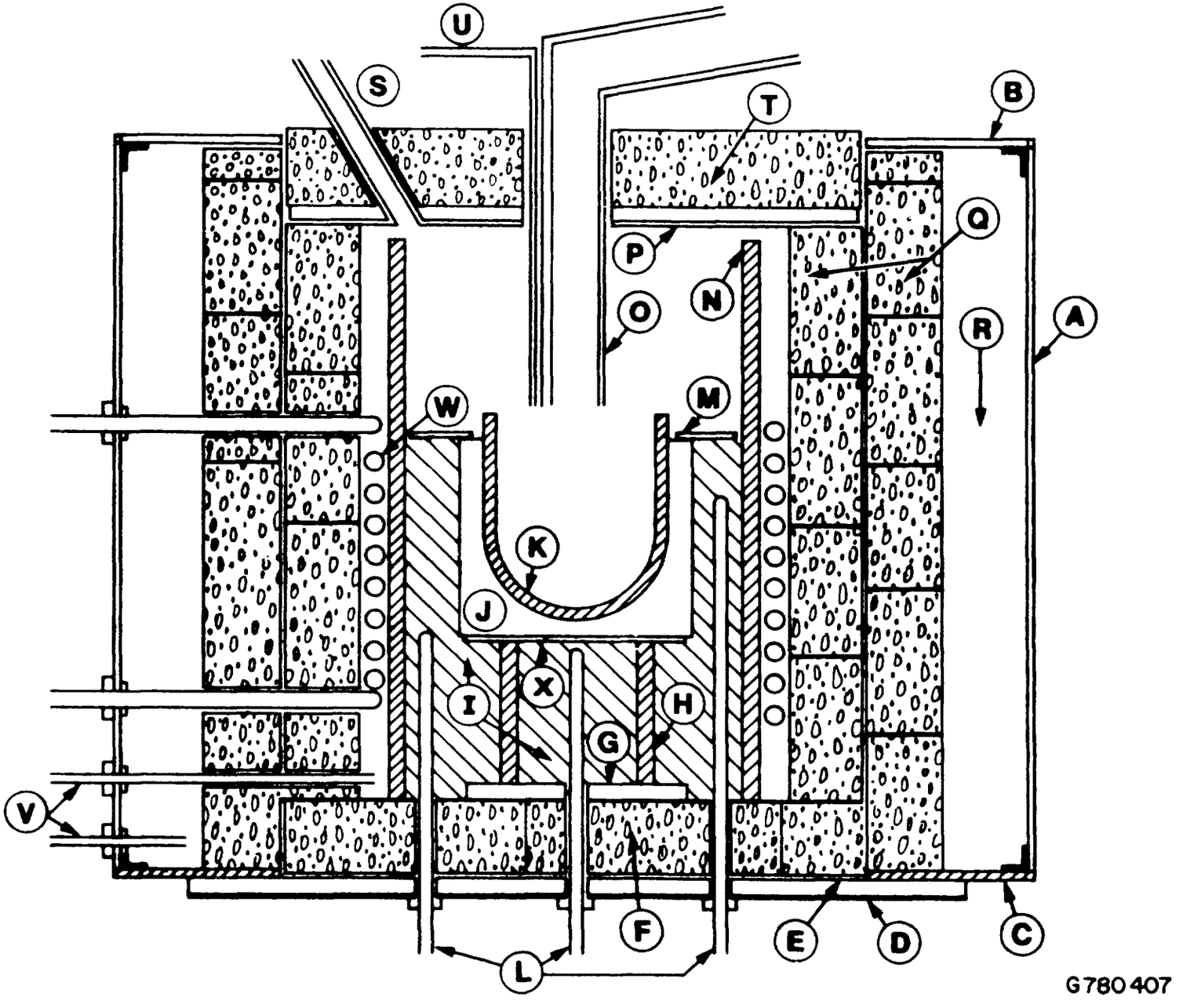

Figure 3 Silicon Melter Schematic.

A Plexiglas chamber 762 mm x 762 mm x 610 mm high 13 mm thick - all joints sealed

B Transite top 6 mm thick w/ 483 mm x 483 mm access opening - rubber gasketed

C Linen-based Bakelite 13 mm thick w/ 483 mm x 483 mm cut out

D Transite base 19 mm thick 660 mm x 660 mm

E "Grafoil,"* 0.4 mm thick, over entire Transite base

F Firebrick base

G Alundum base for pedestal approximately 10 mm thick - 178 mm diameter

H Alumina pedestal 133 mm O.D. x 114 mm high, 10 mm wall

I Carbon felt** insulation

J Susceptor, purified graphite, 178 mm diameter - 152 mm high, accepts a 152 mm diameter crucible

K Quartz crucible - 152 mm diameter - 178 mm high

L Thermocouple wells (3) sealed through Transite base w/ Swagelocks

M "Grafoil" ring 0.4 mm x 152 mm I.D. x 279 mm O.D.

N Opaque quartz 279 mm I.D. x 305 mm O.D. x 457 mm

O Transfer and powder feed tube - 51 mm diameter quartz

P ATJ Graphite 13 mm thick x 476 mm x 476 mm w/ "Grafoil" underside

Q Double walled firebrick w/ staggered joints

R Void area for argon atmosphere

S Alumina sight tube for visual observation and exhaust

T Firebrick insulation

U Argon supply for crucible

V Argon supply for furnace (2) 1 each for inner and outer chamber

W Work coil water cooled 12T 114 mm off base 241 mm long

X Single layer of carbon felt

*"Grafoil" is a registered trademark of Union Carbide Corporation.

**Union Carbide Corporation Grade WDF carbon felt.

Figure 3 Legend

E. Valla 12-13-78

2.2.3b SILICON POWDER COMPACTION

Approximately 300 g of free space reactor powder was sent to Bepex Corporation for a bench test of the compactability of the powder. The powder was die compacted at pressures of 30,000 psi (207 MPa) and 50,000 psi (345 MPa) in its as-received state (no binders or lubricants added). A green density of 45% of the theoretical value was obtained. The silicon powder compacts formed by die pressing without additives, both by Union Carbide Corporation and Bepex Corporation personnel, either split apart or delaminated upon ejection from the die. This indicated that additives would be necessary to obtain uniformly sized compacts. Bepex personnel felt that additives would be required to produce uniformly sized briquettes on their roll press. Without additives, the product would probably resemble the product obtained from die compaction.

Free space reactor powder was isostatically compacted at the Parma Technical Center. Small compacts (38 mm diameter x 203 mm long rubber bag molds) were crack-free and were used to determine the green density as a function of compaction pressure (data shown in Figure 4). One attempt was made to isostatically mold a large (121 mm diameter x 559 mm long mold) compact at 20,000 psi (138 MPa). The compact broke into several pieces. Isostatic pressing of free space reactor powder may be a means of reducing the volume of a given weight of powder to facilitate shipment and storage.

2.3 CONCLUSIONS

It was demonstrated that the free space reactor, storage hopper, and powder melter can be operated as a connected assembly to eliminate manual handling of the powder and its exposure to atmospheric contaminants. Recent

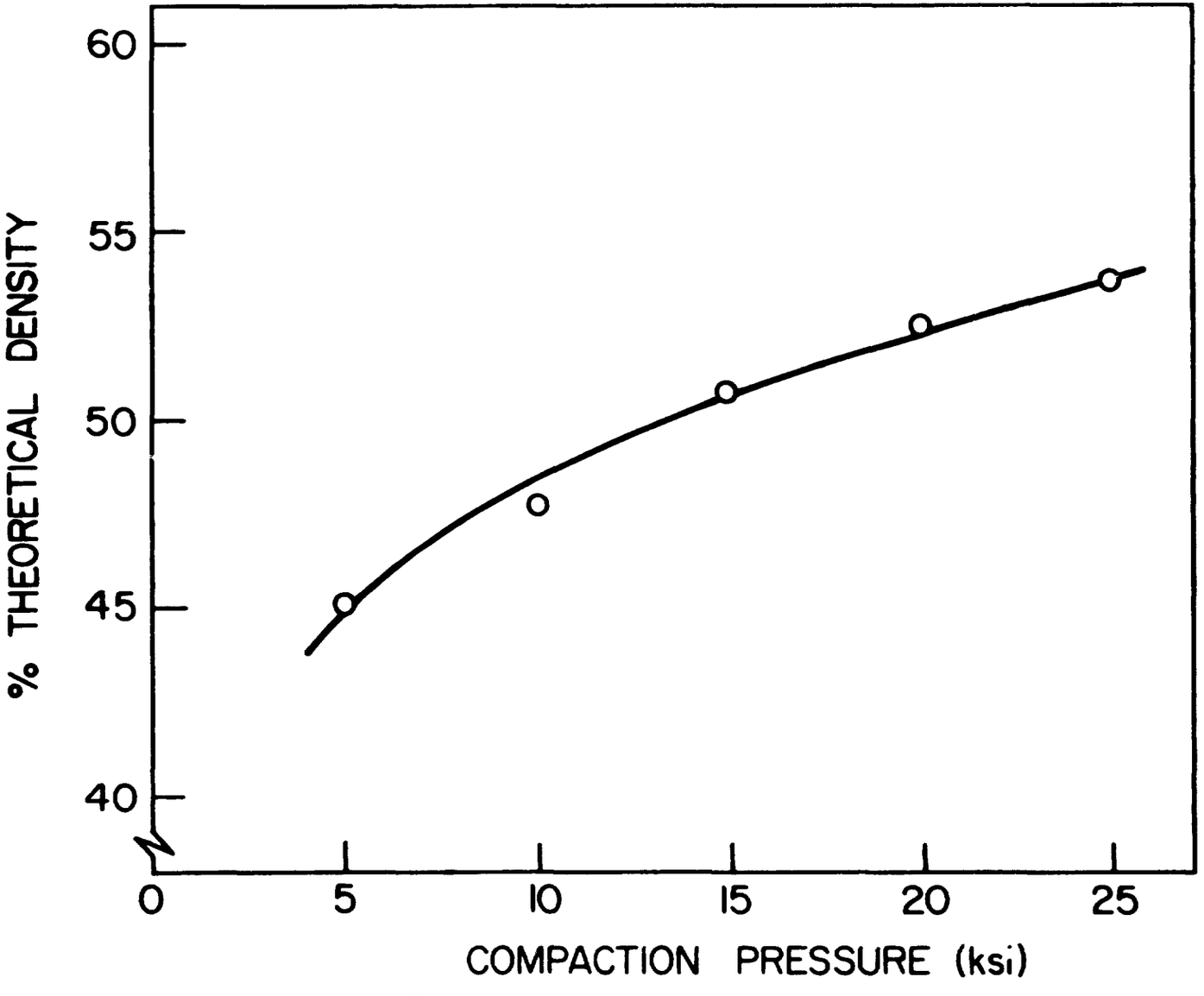

Figure 4 Effect of Isostatic Pressure on Compact Density.

G780410

reactor design and operating procedure modifications effectively prevented powder from accumulating on the reactor lid and on the silane injector. The next step towards achieving long-term operation capability will be to prevent the powder from building-up on the reactor wall. Once this is accomplished, the primary task will be to operate the connected assembly for five (5) consecutive powder production runs.

Die pressing or briquetting without the use of additives will not result in the formation of uniformly sized compacts due to delamination and chipping. The utilizion of this form of product as feedstock for a melter has not been demonstrated. Isostatic pressed compacts may also be used as feedstock for melting.

2.4 PROJECTED FIRST QUARTER, 1979, ACTIVITIES

Continue to minimize the buildup of silicon powder in critical areas of the free space reactor.

Conduct five (5) consecutive powder production experiments in the connected free space reactor assembly. The silicon powder produced in some of the experiments may be melted in 152 mm diameter quartz crucibles.

slz

TABLE OF CONTENTS

TABLE OF CONTENTS (CON'T)

TABLES

ILLUSTRATIONS

FLUID-BED PYROLYSIS R & D

Tests conducted in the cold fluidized bed indicate that the bed can be maintained in a steady, bubbling state at extremely low gas densities; this is in contrast to the opinion of some fluid-bed experts. Stable operation was also attained with a boot section attached to the bottom of the reactor, instead of a distributor plate. However, effective segregation of large particles was not accomplished in the initial experiment. Further tests are needed to learn more about particle segregation.

Capacitive heating of a silicon bed to 500^{o}-900^{o}C was successfully demonstrated. The bed was heated to 785^{o}C and, moreover, a favorable temperature gradient of 12^{o}C between the hot particles and the cold wall was observed. This temperature gradient is desirable to minimize silane pyrolysis on the reactor wall.

Finally, long-term attrition tests at ambient and high temperatures show that the particle attrition is very small as long as particles are dense and coherent.

3.0 PROCESS DESIGN

3.1 INTRODUCTION

This program, started in October 1977, was to provide JPL with engineering and economic parameters for an experimental unit sized for 25 metric tons of silicon per year and a product cost estimate for silicon produced on a scale of 1000 metric tons per year.

Since the experimental unit size was changed from 25 MT/Yr to 100 MT/Yr in early summer of 1978, the unit was officially named the EPSDU (experimental process system development unit). Work in this reporting period focused on the EPSDU process design in sufficient detail for cost estimating and engineering.

A heat and mass balance of major streams was made incorporating as much as possible of the process design data generated in the last quarter. This heat and mass balance is the basis for all subsequent process design activities listed below:

- Equipment functional design and specifications are in preparation.
- Work on a detailed process and instrumentation diagram has started.

- A layout is under preparation which is specifically directed to the EPSDU.
- The waste treatment section was re-examined and a new method centered around thermal oxidation was adopted.
- A preliminary economic study of two proven melting and consolidation systems was made.

The heat and mass balance will be updated at least one more time incorporating updated dichlorosilane and trichlorsilane redistribution equilibrium and kinetic data.

3.2 DISCUSSION

3.2.1 SGS PROCESS DESIGN FOR THE 100 MT/YR EPSDU

3.2.1a Heat and Mass Balance

A mass balance of the major streams for silane production was completed based on the experimental VLE and solubility data generated this year and on literature data. For this task, the process was divided into five parts — the settler system and four distillation columns — in order to calculate the component separation data using the best calculational method for each part. This was detailed in the September Monthly Progress Report. Literature data and ideal VLE calculations were used to compute the mass balance around

Columns 3 and 4 (dichlorisilane and silane distillation columns). Necessary experimental data are being generated for future updating.

Typical enthalpy data used in the heat and mass balance is presented in Figure 3.1 in the form of a Mollier diagram. In constructing the diagram, ideal gas enthalpy was pressure corrected using the Redlich-Kwong equation of state down to the saturation line. At temperatures below saturation temperature, vapor enthalpy was set equal to saturated vapor enthalpy at the temperature. Below the critical temperature, liquid enthalpy was computed by subtracting the latent heat of the components from ideal gas enthalpy (See Figure 3.2). Latent heat is computed by the Clausius-Clapeyron Equation. Broken lines in the figure indicate the old data which is shown for comparison. The enthalpy correlation in this figure and similar correlations were used to generate a heat and mass balance of the entire process except for distillation simulations, where no pressure correction was made. Errors resulting from this were small — in the order of one to two percent.

3.2.1b Stream Catalog and Process Flow Diagram

A preliminary stream catalog was prepared based on the heat and mass balance of major streams described in the previous section. The catalog does not

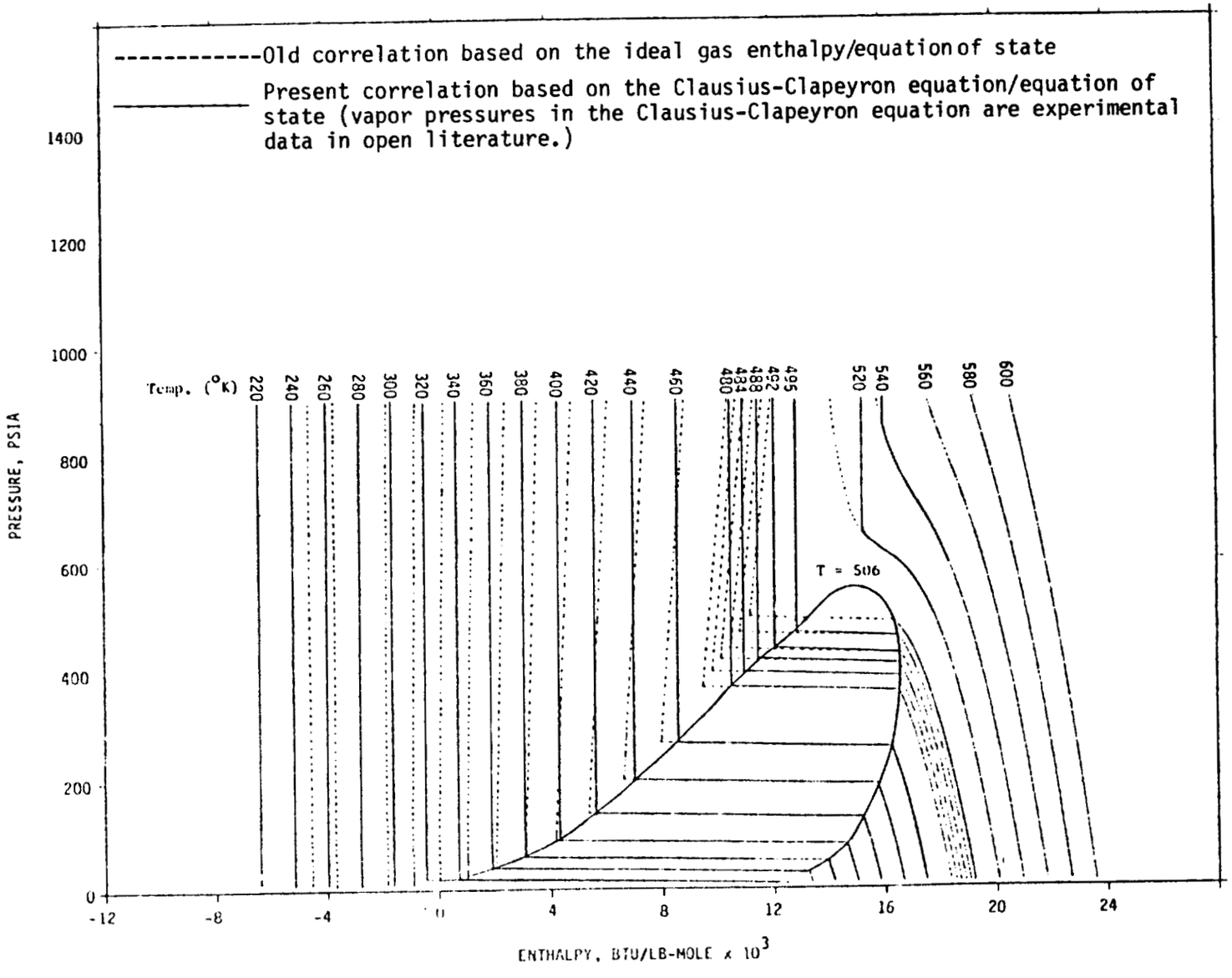

FIGURE 3.1 MOLLIER DIAGRAM FOR STC

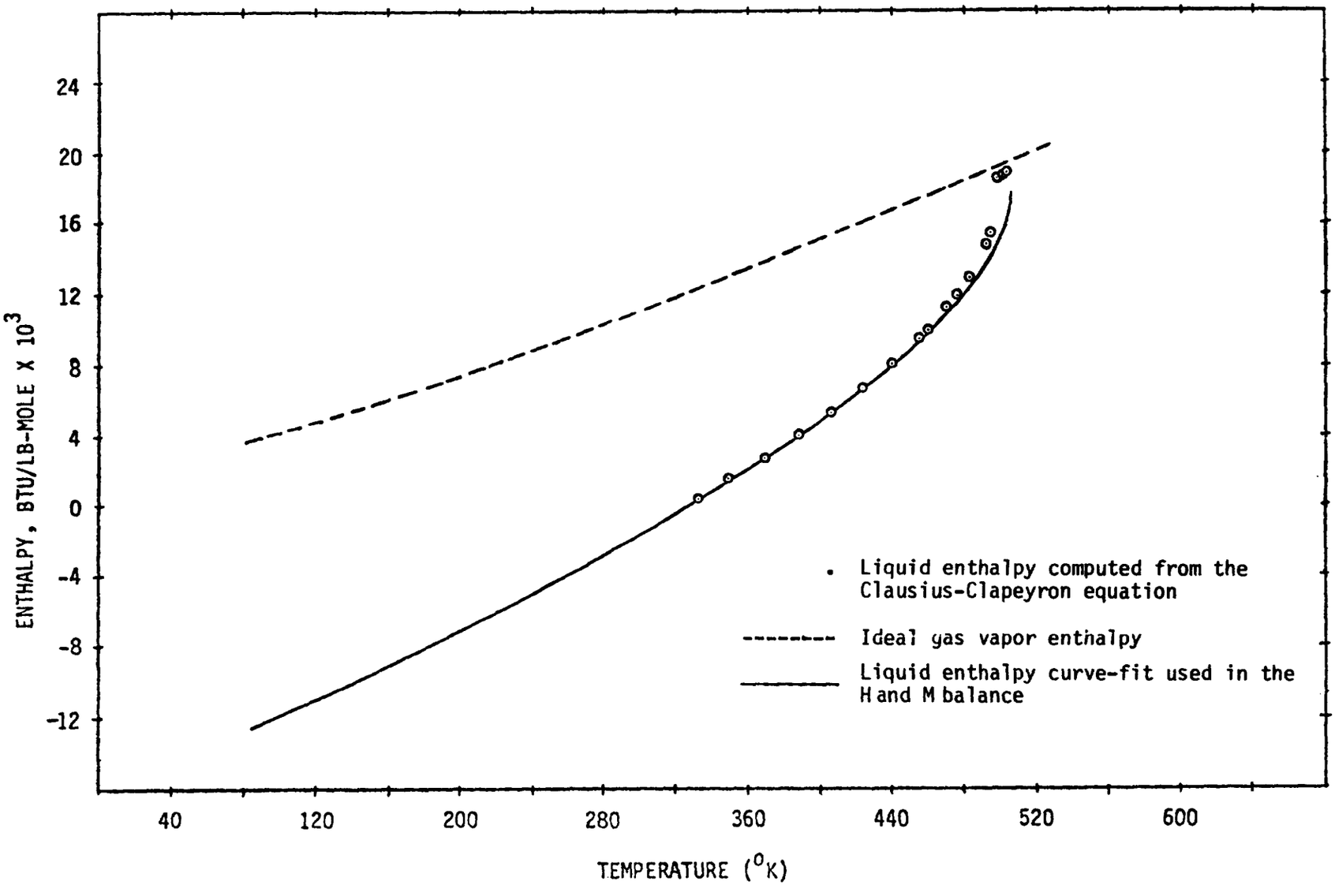

FIGURE 3.2 IDEAL GAS ENTHALPY CURVE FIT FOR SILICON TETRACHLORIDE

include trace components which will be incorporated later. The stream catalog provides three basic stream data: (i) a summary of all streams; included are the stream number, stream description, temperature, pressure and liquid fraction; (ii) thermophysical properties of all components that exist in the process; and (iii) a stream-by-stream compilation of pressure, temperature, liquid fraction, enthalpy, heat of formation, average molecular weight, stream composition, and elemental composition.

The corresponding process flow diagram (PFD) is presented in Figures 3.3 through 3.6. The PFD is divided into four sections: Section I - Hydrogenation, Section II - Distillation/Redistribution, Section III - Pyrolysis/Consolidation, and Section IV - Waste Disposal. Stream numbers in the PFD correspond to those in the stream catalog. Since the PFD was prepared, the waste disposal method was extensively revised from chemical oxidation to thermal oxidation as presented in Paragraph 3.2.2 of this report. The PFD will be updated in the next quarter incorporating this and other process improvements.

3.2.1c Process and Instrumentation Diagram and Layout

P & I worksheets for all four sections were prepared which feature a conventional pneumatic control

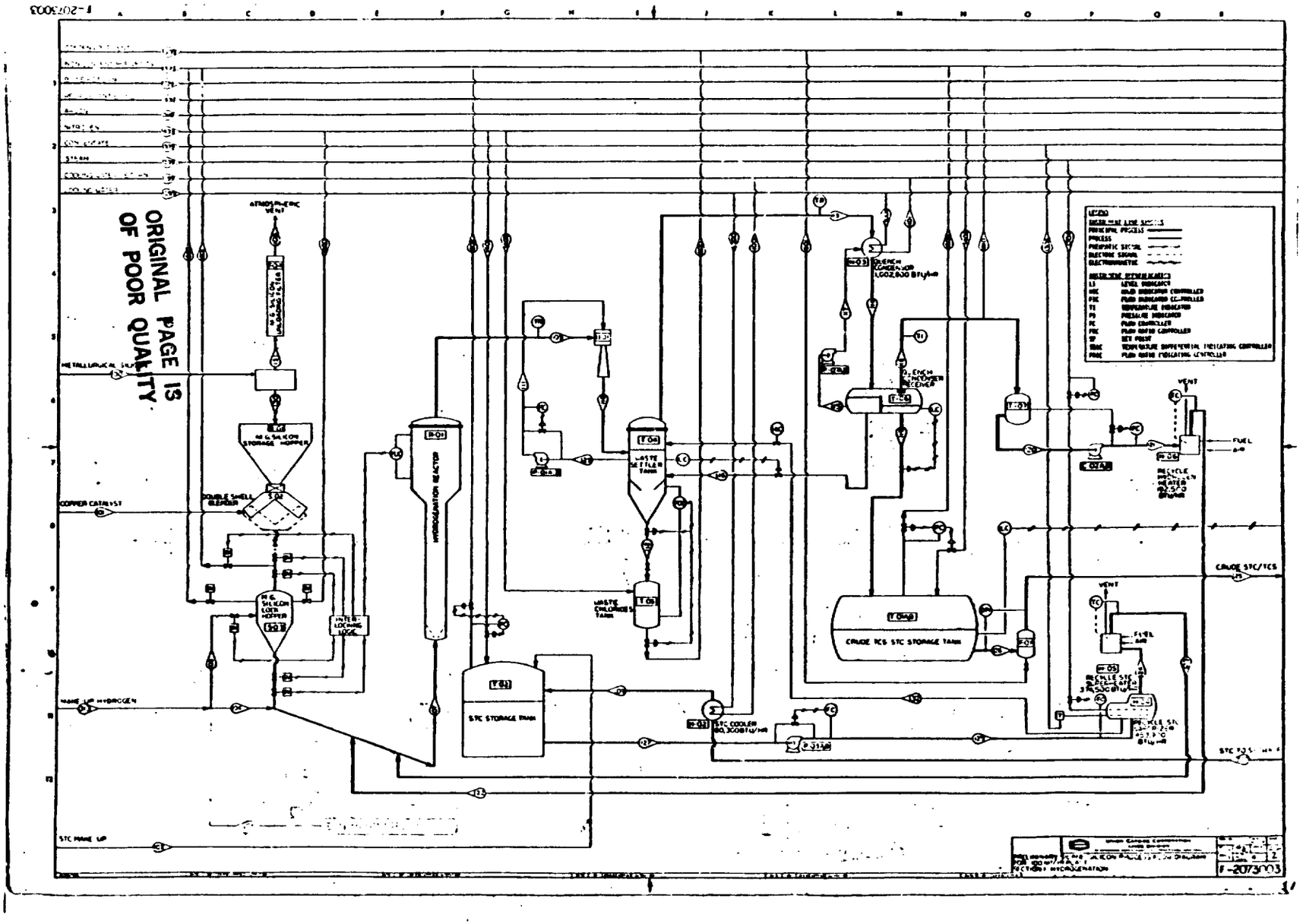

FIGURE 3.3 PRELIMINARY SILANE/SILICON PROCESS FLOW DIAGRAM FOR 100 MT/YR FACILITY - SECTION I: HYDROGENATION

ORIGINAL PAGE IS
OF POOR QUALITY

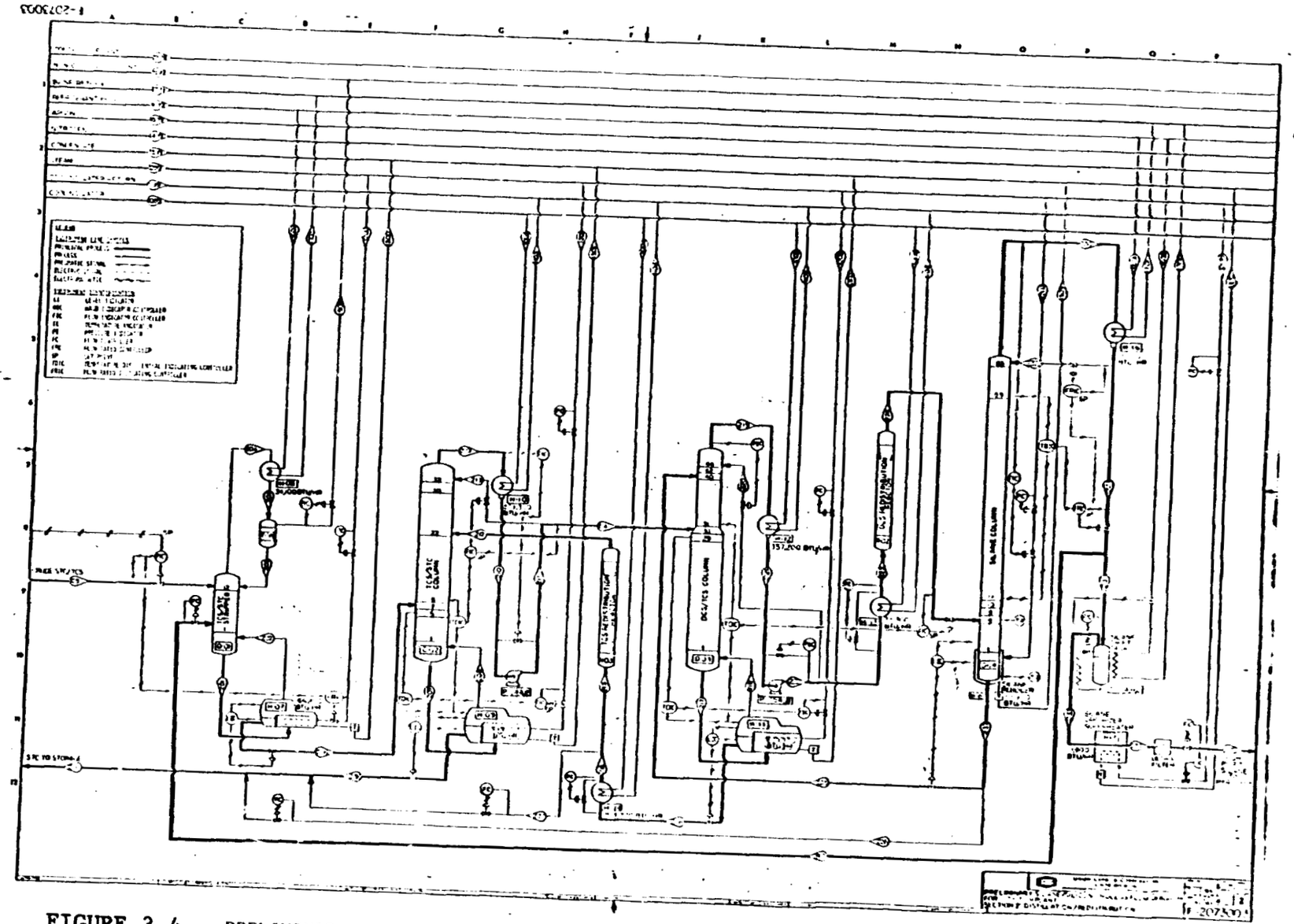

FIGURE 3.4 PRELIMINARY SILANE/SILICON PROCESS FLOW DIAGRAM FOR 100 MT/YR FACILITY - SECTION II: DISTILLATION/REDISTRIBUTION

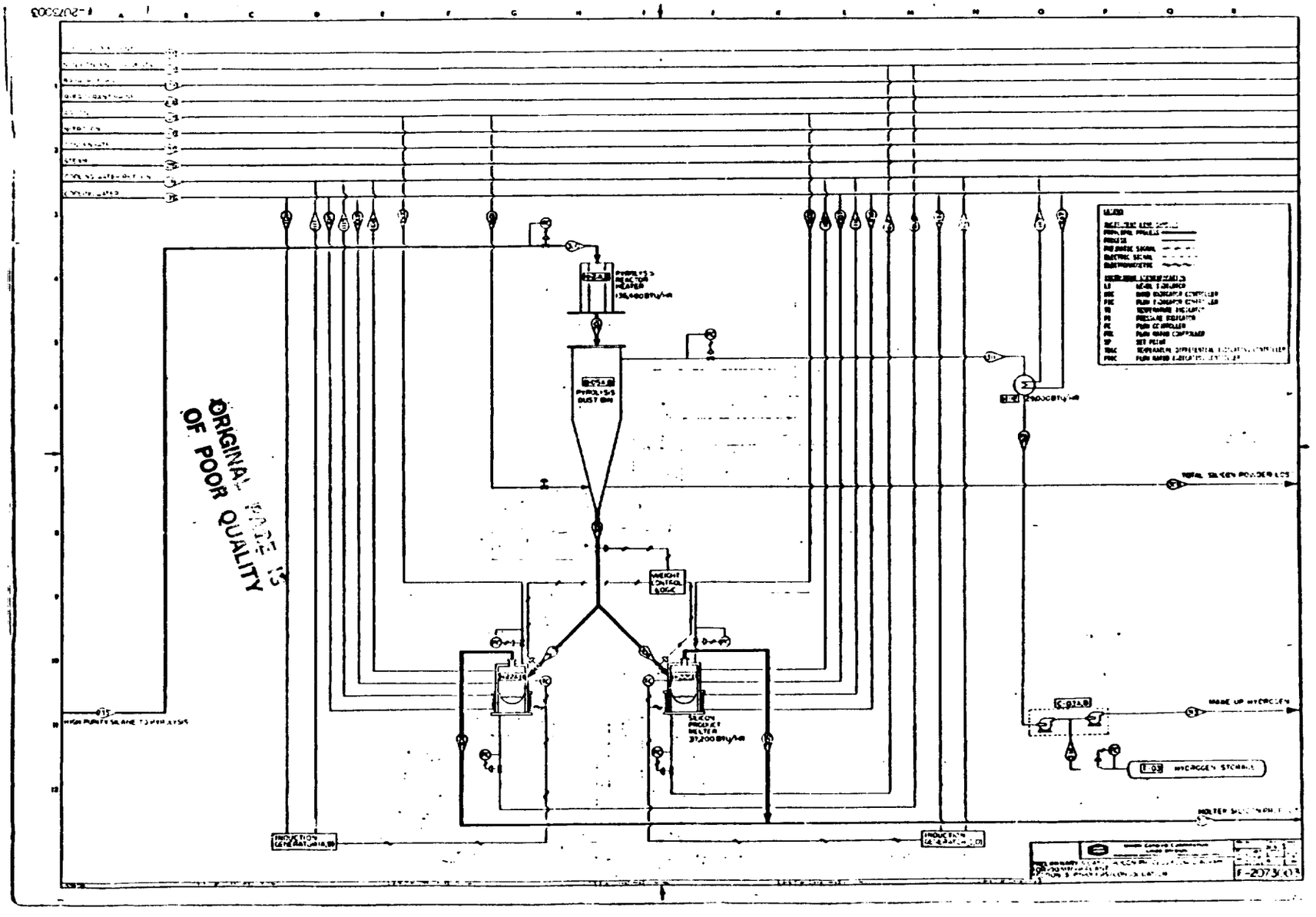

FIGURE 3.5 PRELIMINARY SILANE/SILICON PROCESS FLOW DIAGRAM FOR 100 MT/YR FACILITY - SECTION III: PYROLYSIS/CONSOLIDATION

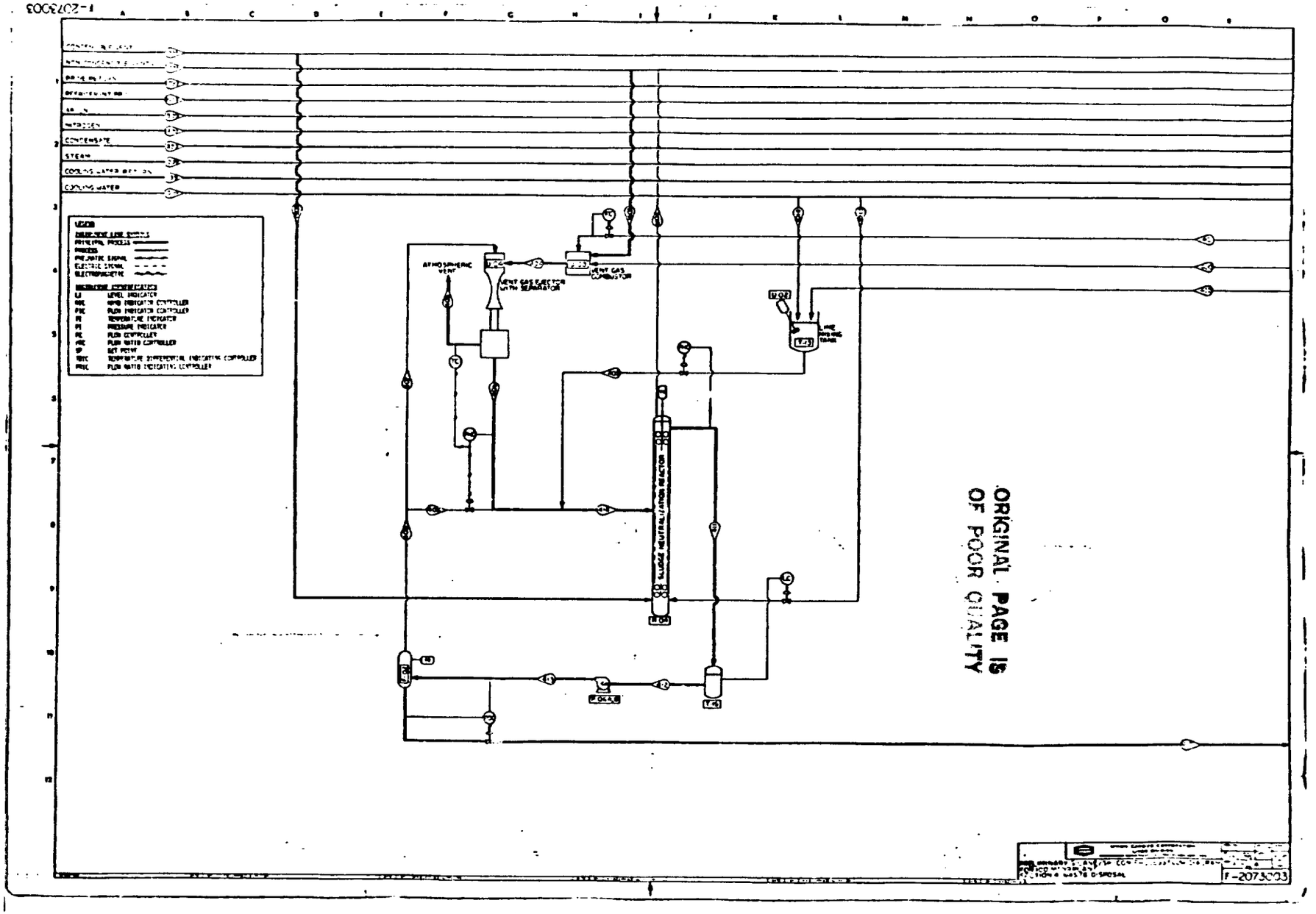

FIGURE 3.6 PRELIMINARY SILANE/SILICON PROCESS FLOW DIAGRAM FOR 100 MT/YR FACILITY - SECTION IV: WASTE DISPOSAL

scheme with a data collection computer. In preparing the P & ID, efforts were initiated in contacting instrument vendors and in studying control and instrument schemes of existing UCC plants having processes similar to the proposed silicon facility. This effort will culminate in the P & ID which illustrates all valves, actuators, instruments and control lines.

A layout for the EPSDU is under development. Because of the experimental nature of the EPSDU, most equipment is installed indoors, while the 1000 MT/Yr commercial plant layout made in February 1978 was essentially for an outdoor installation. Work is underway to determine the best equipment arrangement and to use temporary structures or rental housing such as trailers, wherever possible.

3.2.1d Redistribution Reaction Computer Program

The computer program which is utilized in the evaluation of the redistribution kinetic data was developed in August 1978. Trichlorosilane and dichlorosilane redistribution data recently provided by the Sistersville facility indicates strong kinetic dependency on the fluid velocity in the catalyst bed suggesting combined diffusion

and second-order surface resistance. The computer program system is being modified to include diffusion resistance after which it will be used to reduce the liquid phase experimental raw data now available.

3.2.1e Waste Disposal Experiments

Disposal of waste sludge containing metal chloride in chlorosilane may be accomplished in two ways. The first method uses treatment by acid hydrolysis and lime neutralization. The second approach uses thermal oxidation in a combustion chamber.

Thermal oxidation is used to treat silane process waste in our Keasbey plant. In this treatment process, the combustion effluent is scrubbed with water to remove particulates from the effluent gas. The water, after scrubbing, is brownish and contains fine silica particles. These particles are so fine that filtering through paper, which captures particles greater than 2 microns, removes only a small fraction of the solids and the filtrate still has a brown color. However, when the pH of the water sample was increased to 11.5 and greater, immediate precipitation occurred. Subsequent heating to 80^{o}C caused particle size growth and the sample liquid became clear. Filtering removed all solids.

A test apparatus, which treats liquid wastes by chemical oxidation with lime (the first scheme), was built and tested. Water is added to STC in the first stage of the test reactor which produces silicon and HCl. Water helps agglomerate silica particles making them easy to filter out. Lime is added at a later stage to neutralize the solution. One experimental run was made which proved that STC can be neutralized with lime and the silica was filtered out of the neutralized solution. However, once the STC flow was stopped, the flow could not be restarted because of the formation of a plug around the STC inlet check valve. Subsequent runs with a reduced STC throughput did not eliminate plugging. It was found that a small nitrogen purge stream is needed in the STC line during the STC hold periods. The purge stream was able to keep the line free of water and thus prevented formation of silica plugs.

Presently, we plan to process liquid wastes through thermal oxidation in a combustion chamber, and the liquid-phase chemical oxidation method being tested now will serve as an alternate with further development.

3.2.2 SGS EQUIPMENT FUNCTIONAL DESIGN AND SPECIFICATIONS FOR THE EPSDU

3.2.2a Hydrogenation Reactor Design

Based on the heat and mass balance described in paragraph 3.2.1a, conceptual design of the hydrogenation reactor was made for the EPSDU. It is a fluid-bed reactor containing metallurgical-grade silicon powder with a mean particle diameter of 200 microns, and it has an operating fluidization velocity of 0.2 ft/sec. The bed is 20 inch I.D. with an expanded head of 34 inch I.D. at the top which serves to disengage small particles from the gaseous effluent. A sketch of the reactor is shown in Figure 3.7.

3.2.2b Distillation Column Design

Based on the heat and mass balance of major streams, functional design of the four distillation columns for the EPSDU was completed. The column sizing and tray design are based on the theoretical tray count, multi-component, multi-separation simulation process computer program (MMSP) available in-house. Although a conservative approach has been taken, the design philosophy for the trays follows the same design criteria and guidelines as other multi-component distillation columns designed commercially.

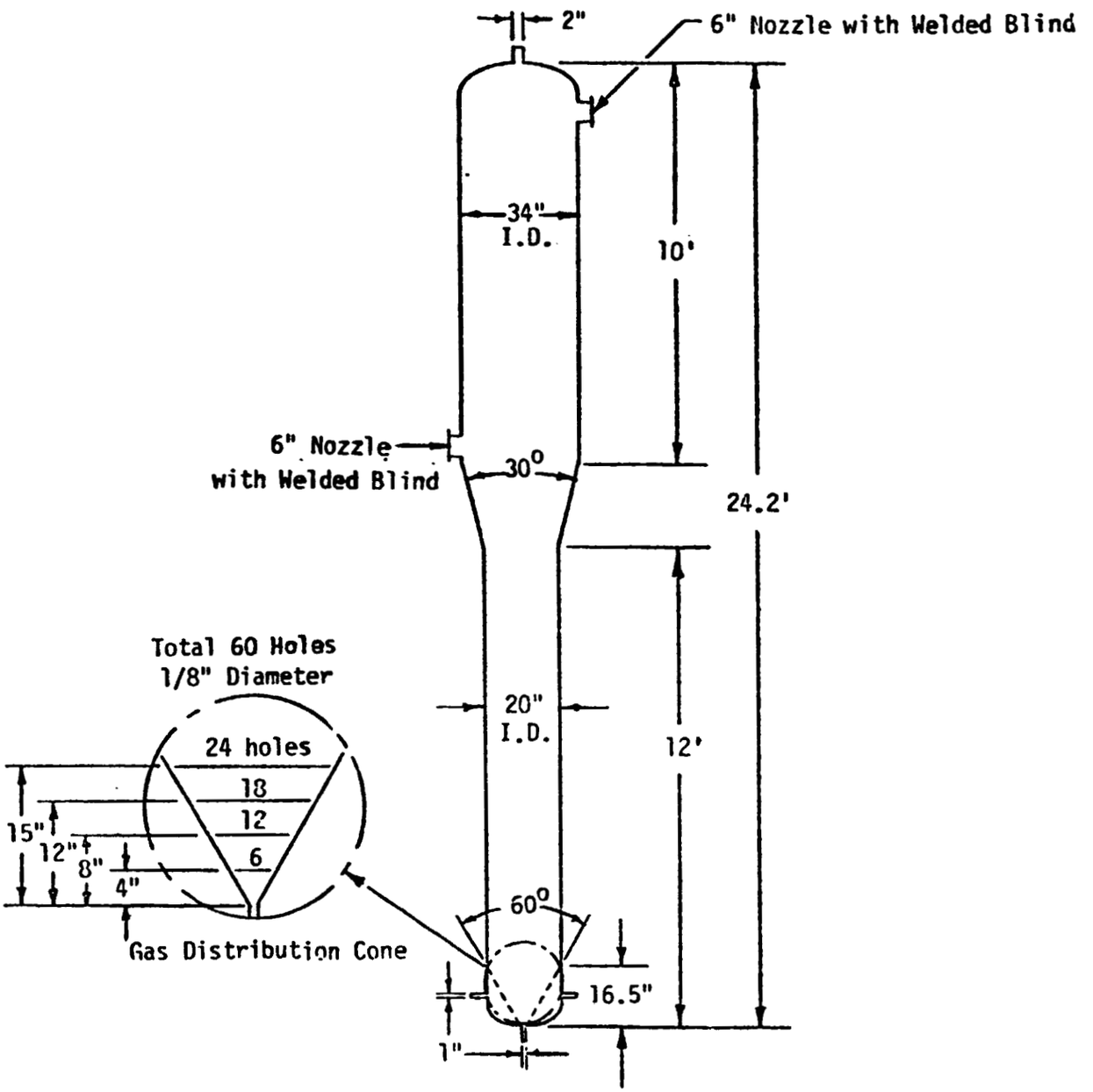

FIGURE 3.7 HYDROGENATION REACTOR FOR EPSDU

The column performance was rated at the design load as well as at 70 and 100 percent of the design load. All columns were found to perform well with good separation efficiencies at these off-design loads. Figure 3.8 presents the relative sizes of all four distillation columns along with key design parameters. As shown, the column diameter ranges from 8 inches to 24 inches and the column height from 27 feet to 55 feet.

Some kinetic and VLE data are still lacking for Columns 3 and 4. Therefore, design of these two columns may change when these data are incorporated.

3.2.2c Melting/Consolidation Design

The EPSDU considered so far had two identical full-sized free-space reactors, one being a spare, and five identical melters, two being spares. Since the EPSDU is an experimental facility and is not intended to be a production plant producing polycrystalline silicon rods every day at full capacity, we decided to install only one full-sized free-space reactor and at most two melters. We believe that this reduction in the number of identical equipment will have a negligible effect in proving the attractiveness of the EPSDU process and will provide a substantial saving in facility and operating cost.

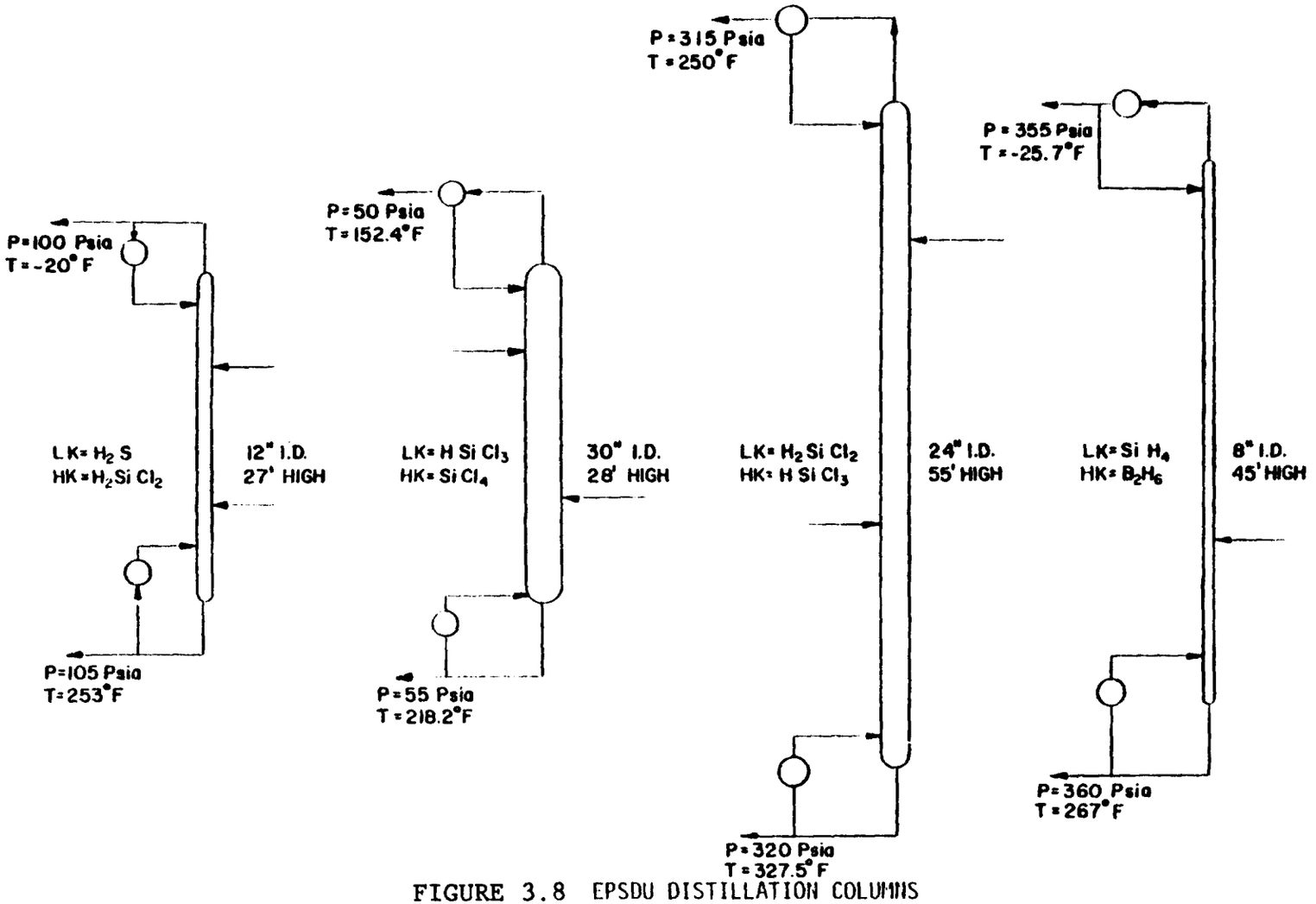

FIGURE 3.8 EPSDU DISTILLATION COLUMNS

Time and motion sequences for the suction-casting steps were analyzed, and the results show that the complete casting steps take about one-half hour. If four 1-inch diameter by 36-inch long rods can be cast simultaneously, 4.5 kg/hr of polycrystalline silicon rods can be produced by each melter. On the other hand, if a 3-inch diameter by 36-inch long rod is produced in one casting cycle the production rate will be about 6 kg/hr.

Vendor contacts for the melter convinced us that a commercial Czochralski single-crystal growing apparatus can be modified to accept silicon powder as a feed and to provide for suction-cast polycrystalline rods. The melter for the EPSDU will be developed jointly with one or two melter vendors. It is desirable to make quartz tubes for suction-casting so that their inside diameter is smooth and slightly tapered. These features should facilitate removal of solidified poly-rods from the tubes. Quartz-tube vendors were contacted to determine the possibility of manufacturing quartz tubes with tapered inside diameters. Some R & D work is required, if we are to pursue this route.

Polycrystalline rods can also be produced by the single-crystal growing technique by quickly pulling the rod from the melt. This rapid-pulling technique may be as cost effective as the suction-casting method, so the economics involved in this technique was investigated and is presented in paragraph 3.2.3. One technical advantage of rapid-pulling over suction casting is that the product should be purer.

3.2.2d Waste Disposal System Design

The process waste treatment system, adopted in the preliminary process design package for a 25 MT/Yr semiconductor-grade silicon experimental facility issued on April 28, 1978, neutralized liquid wastes in a multi-stage mixing column and combusted gaseous wastes in a furnace. This treatment system disposes metal hydrides as land-fill and flue gas to the atmosphere after silica scrubbing. This treatment system is becoming increasingly more difficult to implement because of tighter environmental regulations on chemical landfill.

Consequently, an alternate waste disposal system has been under study which appears superior to the original system and which has, therefore, been selected as the disposal method for the EPSDU. This process flame-oxidizes all wastes and recovers silica and HCl as marketable by-products. In this combustion process, gaseous wastes are incinerated in an open flame burner that fires int- a conical receiver. A vacuum pulled on the receiver draws in the flame and quenches it in a large excess of air. Upon cooling to approximately 300^{o}F, the silica produced in the flame agglomerates to form particles which are removed in bulk by bag filters or cyclones. Silica solids (fumed silica) are removed periodically from the bag filters and heated to 700-800^{o}F in an air stream to desorb

HCl from silica which is then collected in paper bags for final disposition. After filtration, trace amounts of silica are removed by contact in a high-energy venturi. The venturi off-gas then proceeds to an HCl adsorption system to produce muriatic acid. Thus, the process by-products are fumed silica and muriatic acid which are marketable although their value is low. The process is shown in Figure 3.9.

Certain aspects of this process are important for its success:

- Flame Temperature - This affects the size of silica particles, 2000°F is recommended because higher temperatures produce fine particles with attendant filtration problems.
- Rapid Quenching - The combustion product should be quenched rapidly so that fine silicon particles agglomerate, making them easy to filter.
- Steam Dew Point - Solid bearing streams should be maintained above the stream dew point. This is important not only from a corrosion viewpoint, but also due to the hydration of silica to form non-filterable gel.
- Dead-ended Scrubber - A dead-ended venturi scrubber is needed to maintain the low silica level in the muriatic acid necessary to make it marketable.

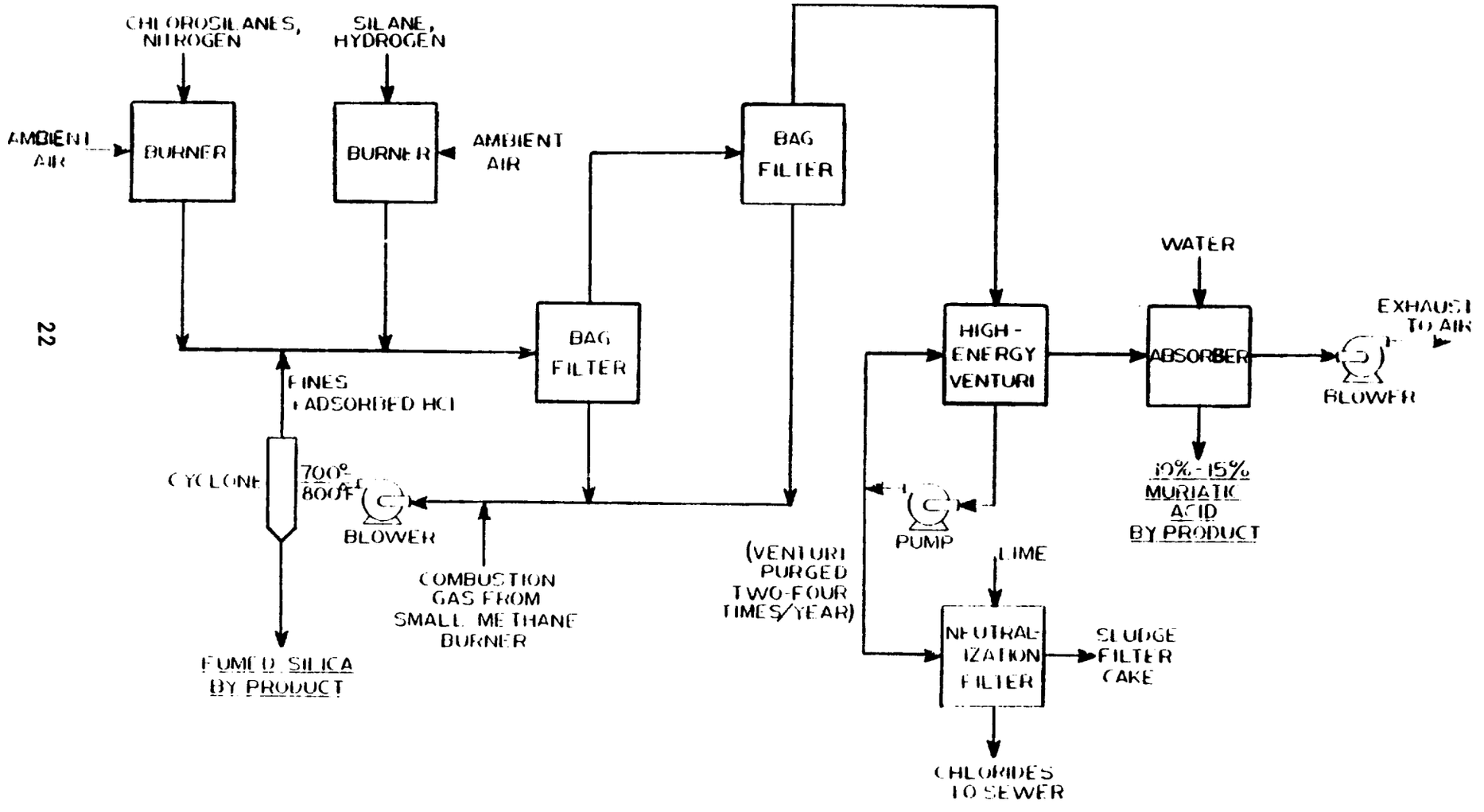

FIGURE 3.9 Schematic Process for Waste Gas Disposal by Combustion

A similar method will be used to cumbust liquid waste; however, some development work would be required to optimize the burner geometry to achieve complete liquid oxidation and avoid deposition of solid silica deposits on burner parts.

The process flow diagram (Figure 3.6) is being revised to reflect the change in the waste treatment method.

3.2.2e Equipment Functional Specifications

Equipment specifications for the EPSDU are under preparation and should be completed by mid-January. Over 90 pieces of process equipment, not counting duplicates or similar items, will be specified. Specifications shall contain sufficient data to allow vendor evaluation and quotation.

Some of the equipment is quite unique to our process, so specifications for items like the pyrolysis reactor shall include detailed drawings. These specifications are based on the most recently completed heat and mass balance dated October 1978.

3.2.3 OTHER ACTIVITIES

3.2.3a Silicon Consolidation Economics

A comparative economic study was made on two methods of silicon consolidation, namely suction casting and rapid pulling of polycrystalline rods at a commercial production rate of 1000 MT/Yr. These two methods of silicon solidification were chosen for study because their technologies are relatively mature and should be ready for the EPSDU.

Of the two methods, the suction casting technique was developed at our Parma facility in the early sixties when casting of 1-inch diameter by 4-foot long rods was demonstrated. More recently, under the present JPL program, 3/4-inch diameter by 1-foot long rods were suction-cast at Parma. As the design stands now, suction casting is labor intensive and likely consumes large quantities of expensive quartz tubes. Nevertheless, it has been considered for consolidation of free-space pyrolysis powder in the EPSDU because it has been demonstrated. For a commercial plant, large diameter rods, typically 3-inch diameter by 3-foot long, need to be cast and the quartz tubes must be reusable to reduce the operating cost. The quartz tubes have a tendency to break while withdrawing the rods with the current technology.

On the other hand, rapid pulling of polycrystalline silicon rods can be accomplished in a standard Czochralski crystal pulling machine. The pull rate depends on a number of factors, but the primary one is the temperature gradient in the solid crystal at the growth interface. There is a theoretical maximum for the growth rate set by the rate of heat removal from the interface by the crystal. [3.1, 3.2, 3.3] A single crystal 4 inches in diameter can be pulled at a rate of 4 inches/hour. A higher pull rate can be expected if a poly-rod is produced. The current practice of discarding the crucible after each pull is very time consuming and expensive. Processing multiple charges from a single crucible is being developed under JPL funding at Hamco, Siltec, and TI. For this reason, the present economic analysis assumes that multiple rods are pulled during a crucible life of 70 hours.

The process sequence and time requirements were developed for the suction casting and the rapid pulling techniques as shown in Table 3.1. The table was constructed based on in-house work, literature on crystal pulling[3.4] and also on conversations with a crystal pulling equipment manufacturer. It shows that the net consolidation rate is approximately 6 kg/hr for suction casting and 2 kg/hr for rapid pulling. For a commercial plant producing 1000 MT/Yr (136 kg/hr) of polycrystalline silicon rods, 23 melters for suction casting and 68 crystal pullers for rapid pulling are required. For the preliminary economic analysis, the following assumptions were made;

TABLE 3.1

MELTING/CONSOLIDATION

PROCESS CYCLE TIME

Suction Casting	Time, Min
Load and Melt	120
Suction Cast	60
Elapsed Time Per Charge	180
23 Recharges/Crucible (180 x 23)	4140
Clean and Crucible Replacing	90
Total Cycle Time	4230 (70.5 hrs)
Throughput: 6 kg/hr/melter	

Rapid Pulling	
Load and Melt	120
Stabilize Temperature	40
Crown Growth	40
Straight Growth	290
Elapsed Time Per Charge	490
8 Recharges/Crucible (490 x 8)	3920
Clean and Crucible Replacing	90
Total Cycle Time	4010 (66.8 hrs)
Throughput: 2 kg/hr/melter	

- 1000 MT/Yr silicon production

corresponds to 136 kg/hour based on 85% overall on-stream capability.

- Labor requirements are one operator

for each melter in the case of suction casting and one operator per 4 pullers in the case of rapid pulling.

- Average power consumption is 50KW

for both suction casting and rapid pulling operations. Electrical power is $0.03/KWH.

- Melt-rate of free-space pyrolysis

powder is approximately 10 kg/hr which is the observed melt-rate for poly rod.

- Economic model is based on 15-

year project life, 10 year sum-of-digits depreciation, 48% federal income-tax, 100% equity financing, 2 years construction time 25% DCF rate.

Since the operating cost for suction casting is a strong function of quartz tube usage, two cases were considered. In the first case, only one rod can be cast from each quartz tube. While, the second case assumes it is possible tc cast two rods from each tube. The estimated investment and annual operating costs are summarized in Table 3.2. The lant investment for rapid pulling is much higher than suction casting, but the reverse is true for the annual operating cost. Table 3.3 summarizes the comparative economics

TABLE 3.2

1000 MT/YR SILICON CONSOLIDATION
INVESTMENT & OPERATING COSTS (1978 $)

Plant Investment:

	Suction Casting	Rapid Pulling
No. of Units	23	68
Estimated Unit Cost	$100,000	$125,000
Total Investment	$ 2.3MM	$ 8.5MM

Annual Operating Cost, $MM:

	Suction Casting		Rapid Pulling
	1 Rod/Tube	2 Rods/Tube	
Quartz Tubes	6.44	3.58	-
Quartz Crucibles	0.27	0.27	0.79
Labor	1.41	1.41	1.04
Power	0.22	0.22	0.66
Argon	0.43	0.43	1.31
Cooling Water	0.05	0.05	0.14
Annual Operating Cost	8.82	5.96	3.94

TABLE 3.3

1000 MT/YR SILICON CONSOLIDATION
PRELIMINARY ECONOMIC ANALYSIS SUMMARY

	$ MM		
	Suction Casting		Rapid Pulling
	1 Rod/Tube	2 Rods/Tube	
Investment	2.30	2.30	8.50
Annual Operating Cost	8.82	5.96	3.94
Working Capital (30% operating cost)	2.65	1.79	1.18
Start-up cost (10% Investment)	0.23	0.23	0.85
Estimated Consolidation Price*:			
1978 $/kg	11.58	8.31	10.0
1975 $/kg	9.57	6.87	8.26

* 15-year project life, 10-year sum-of-digits depreciation, 48% Federal Income Tax, 100% equity financing, 2 years construction time, 25% DCF rate.

of suction casting vs. rapid pulling on a 1000 MT/Yr scale. In 1975 dollars, the projected consolidation prices are $6.87/kg to $9.57/kg for suction casting (two or one rod/quartz tube) and $8.26/kg for rapid pulling.

Neither consolidation techniques at present are cost-effective for meeting the DOE/JPL 1968 goal of $10/kg overall cost of solar-grade silicon. Other consolidation methods such as fluid-bed silane pyrolysis, molten silicon shotting, etc., should be considered for development. It is our plan in the next phase to work closely with commercial silicon puller manufacturers and to continue to develop present and more attractive consolidation method(s) for the EPSDU.

3.3 CONCLUSIONS

A heat and mass balance for the EPSDU was prepared which incorporated most of the process design data generated in the last quarter. It is anticipated however that at least one updating is necessary to incorporate more desirable dichlorosilane and trichlorosilane redistribution equilibrium and kinetic data.

Based on the above heat and mass balance, equipment functional design and specifications are being prepared in sufficient detail to enable vendor quotations and evaluation. This activity is expected to be completed in January 1979.

After the heat and mass balance was completed, it became increasingly apparent that the liquid phase oxidation method employed in the waste treatment section would have difficulty meeting stringent future environmental regulations. Consequently an alternate system has been under study which utilizes the thermal oxidation method. This method was adopted for the EPSDU because it combusts all wastes and recovers silica and HCl as marketable by-products while venting clean, flue gas.

In the silicon melting and consolidation area, a preliminary comparative economic study of two nearly state-of-the-art schemes were made. These schemes are suction casting

of large rods and rapid pulling of poly rods. It is clear that more developmental effort is required to meet the 1986 cost goal.

3.4 PROJECTED QUARTERLY ACTIVITIES

3.4.1 Updating of Heats of Reaction

Heats of reaction of three redistribution reactions and hydrogenation will be updated based on the recently acquired experimental data. Based on the updated values, heats of formation of chlorosilanes will be calculated and compared with those given in the JANAF table.

3.4.2 Final Heat and Mass Balance and Process Flow Diagram

The heat and mass balance will be updated for the last time incorporating the new waste treatment system and the updated heats of reaction. The process flow diagram will then be prepared, based on the new heat and mass balance.

3.4.3 Process and Instrumentation Diagram and Layout

A first-cut detailed process and instrumentation diagram (P & ID) for the EPSDU will be prepared. Likewise, a

first-cut detailed layout will be drawn. We plan to optimize the P & ID and layout drawings during the engineering phase of the proposed engineering/procurement/assembly/operation program for the EPSDU.

3.4.4 Economics of EPSDU - Sized Commercial Plant

Because of the experimental nature, the EPSDU sized for 100 MT/Yr of silicon is on-stream only 70 percent of the time. A commercial plant identical in size to the EPSDU will have a higher on-stream factor, thereby, producing roughly 120 MT/Yr of silicon. An additional difference that a 120 MT/Yr commercial plant will produce is a product of liquid silicon while the EPSDU will produce some polycrystalline silicon rods as well as silicon flakes and that the EPSDU will have additional R & D analytical equipment.

Equipment functional design and specifications will be made for the EPSDU first and then they will be modified for the 120 MT/Yr commercial plant. The economic analysis includes the major equipment cost, operating cost, plant investment cost and the product cost.

3.4.5 Overview Cost of 1000 MT/Yr Commercial Plant

The major equipment for this plant will be scaled up from the EPSDU design except for the pyrolysis system.

Due to the melter crucible size limiation (12 inch diameter maximum), there will be fourteen free-space reactor/melter units in a stacked arrangement.

The overview cost analysis of a 1000 MT/Yr commercial plant includes:

- Budget-pricing of major equipment.
- Plant investment by scaling up from the 120 MT/Yr plant cost.
- Operating cost.
- Product cost.

3.4.6 Final Technical Report

The final technical report for Phases I and II will contain the integrated results of all the work performed at al Union Carbide locations.

3.5 REFERENCES

3.1 Ciszek, T. F., J. Applied Physics, Vol. 47, 1976.

3.2 Wilcox, W. R. and Duty, R. L., J. Heat Transfer, Vol 88, 1966.

3.3 Rea, S. M. and Wakefield, G. F., Conference of International Solar Energy Society, Winnipeg, Canada, 1976.

3.4 Lane, R. L., "Continuous CZ Growth," Second Quarterly Progress Report to JPL, January 1 - March 31, 1978.

4.0 FLUID-BED PYROLYSIS R & D

4.1 INTRODUCTION

The purpose of this program is to explore the feasibility of using high-frequency capacitive heating to control the fluidized silicon-bed temperature during the heterogeneous decomposition of silane and to further explore the behavior of a fluid bed. These basic studies will form part of the information necessary to assess technical feasibility of the fluid-bed pyrolysis of silane.

It was shown in this quarter that a silicon bed can be heated to the high temperatures desirable for silane pyrolysis. It was also shown that a stable fluidized bed can be maintained at a low gas density which was thought to be difficult. Since these experimental programs were successfully completed, no more test programs are planned under the current program.

4.2 DISCUSSION

4.2.1 Cold-Bed Fluidization Tests

The purpose of these tests is to aid in establishing the optimum operating conditions for the future silane-pyrolysis PDU. In the PDU, seed silicon particles

will be fluidized by a mixture of silane and hydrogen at temperatures between 600 and 900°C. In order to simplify the experiments, the PDU operating conditions are modelled by a cold bed fluidized by helium at room temperature. For proper modelling, mechanical conditions such as gas viscosities and densities must match in the cold and hot bed. Fortunately, the viscosity of helium at room temperature and that of the silane-hydrogen mixture at high temperatures are similar (2×10^{-5} to 2.6×10^{-5} Pa·s). On the other hand, the density match is possible only by operating the cold bed at reduced pressure. Figure 4.1 shows the helium pressure in the cold bed required to properly model the operating conditions of the PDU at various silane mole fractions and temperatures.

In the tests conducted this quarter, two bed pressures were used — 0.18 (~140 mm Hg) and 0.34 atm (~ 0.260 mm Hg). These cold bed pressures correspond to the silane mole fractions of 0 and 0.067, respectively, at the PDU bed temperature of 900°C. These tests were performed in the 6-inch diameter glass column using bed depths of one, two, and three feet. The results of the test, in the form of gas velocity vs. pressure drop through the bed, are presented in Figure 4.2. The following can be concluded from the test results:

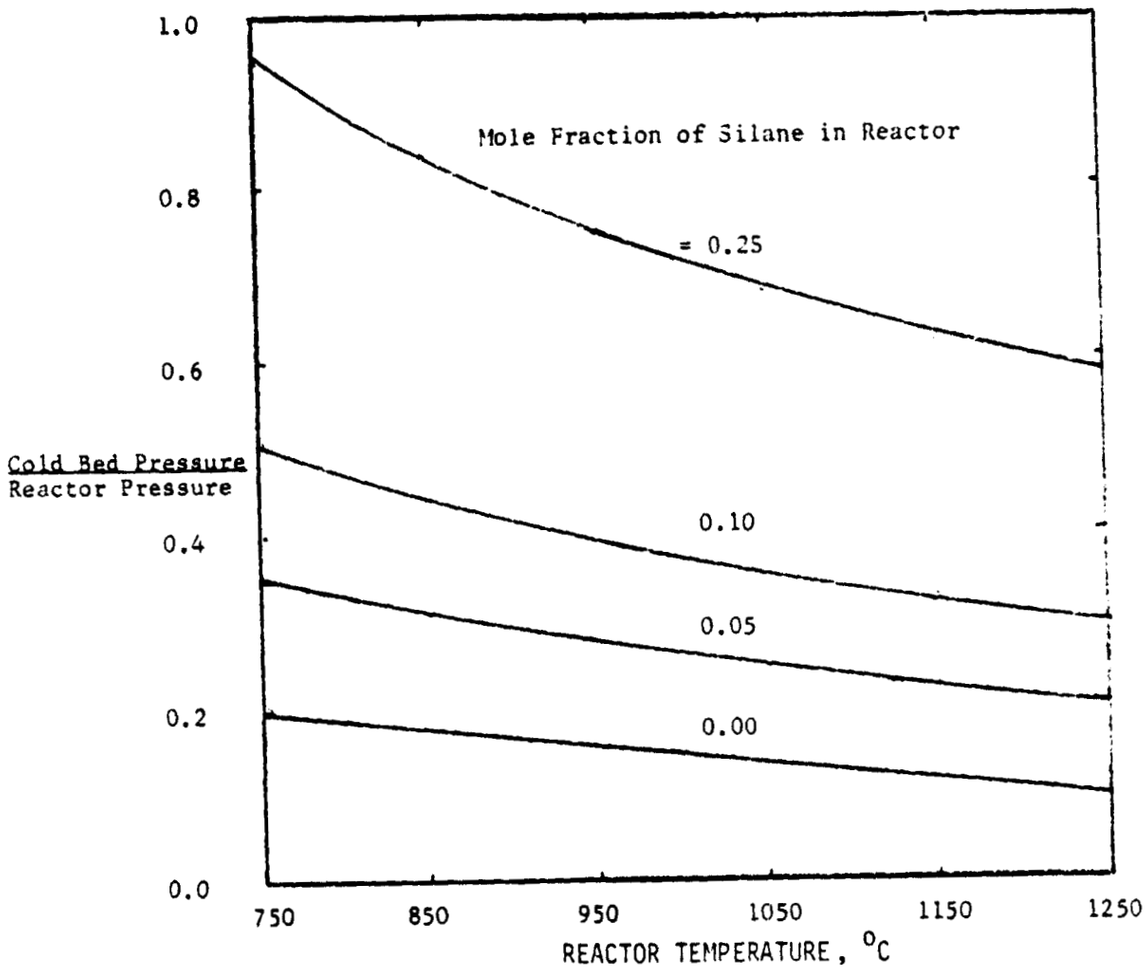

FIGURE 4.1 DENSITY MATCH BETWEEN HELIUM IN COLD BED AND SILANE-HYDROGEN MIXTURE IN HOT BED AT VARIOUS SILANE MOLE FRACTIONS AND TEMPERATURES IN HOT BED.

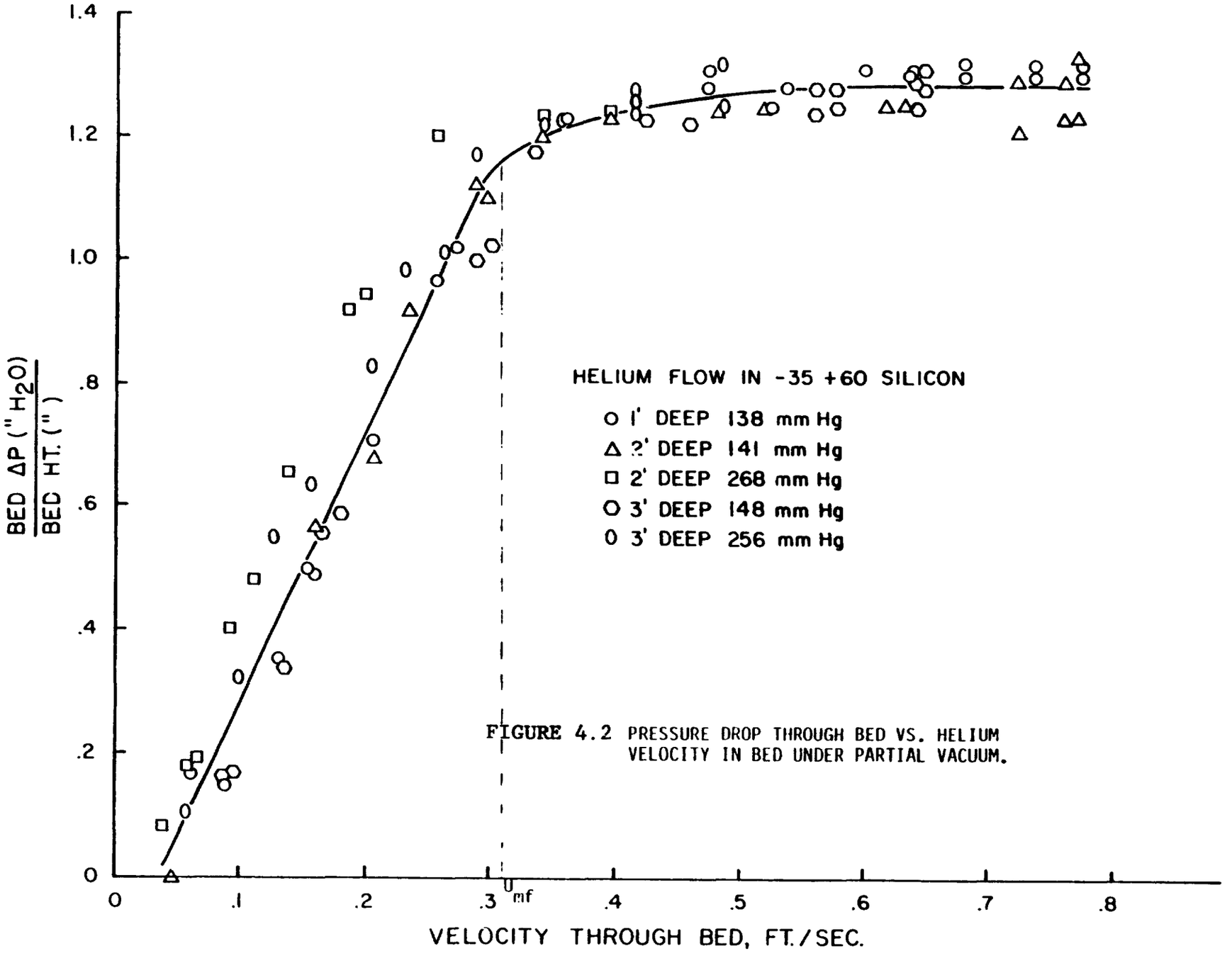

FIGURE 4.2 PRESSURE DROP THROUGH BED VS. HELIUM VELOCITY IN BED UNDER PARTIAL VACUUM.

- There was a speculation among consultants that the bed may not be stable at low gas densities. However, even at the very low gas density in the test bed (0.002 to 0.004 lbm/cu. ft.), the bed can be operated without slugging up to gas velocities twice the minimum fluidization velocity.
- The effect of gas density on the bed behavior is not as strong as expected.
- A stable bubbling bed can be maintained in the 6-inch diameter column with bed depths of one, two, and three feet.
- These tests were conducted using a sintered metal distributor. In the PDU, a boot section will be added in which the product is separated from the seed particles.

4.2.2 Attrition Tests

These tests were conducted to determine the rate of attrition of silicon particles in a fluid bed made of a 1-inch diameter glass tube. The rate of attrition is important because a large amount of attrition diminishes the product yield while a small attrition rate may be desirable in generating seed particles.

Tests at ambient temperature with high-purity silicon particles fluidized by nitrogen were completed. The attrition rates, measured with two particle-size distributions at U/U_{mf} of 2 and 5, are given in Figure 4.3. The conclusions from the tests results are:

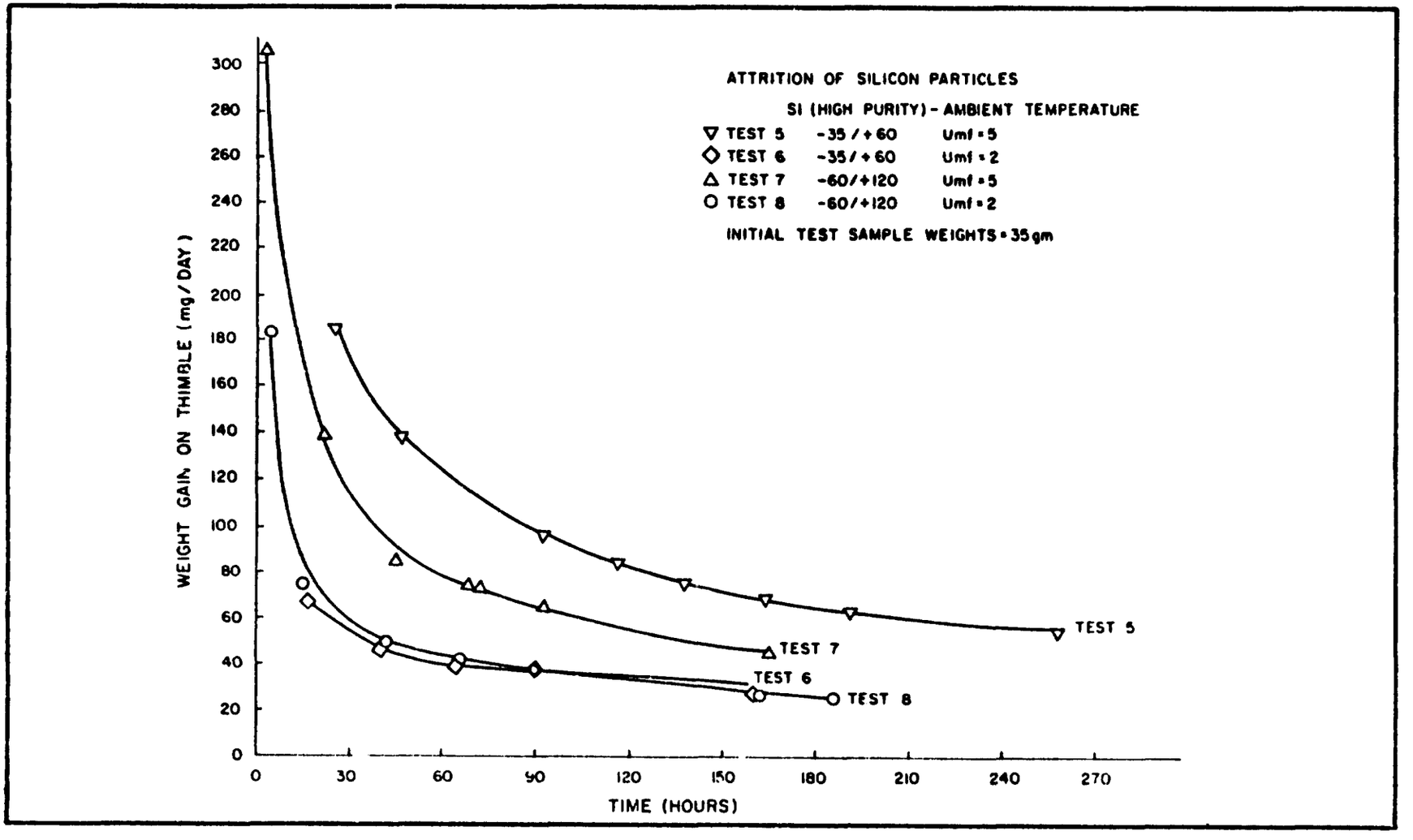

FIGURE 4.3 RATE OF FINES GENERATION FOR SEMICONDUCTOR-GRADE SILICON PARTICLES AT U/U_{mf} = 2 AND 5

- For dense, coherent particles, the attrition rate is very slow. After a high initial attrition period, attrition losses decline to 0.3 percent of bed weight per day.
- These losses are a small fraction of the expected weight gain due to silane pyrolysis.
- These results may not apply if the particle surface is porous. Attrition tests with porous particles will not be performed in this phase of the program.

High purity silicon was also fluidized at a U/U_{mf} of about five and at 600°C in the 1-inch quartz tube attrition tester. After 72 hours of initial operation, a substantial amount of fine brown powder deposited on the tube wall and in the filter. Subsequent operation, after cleaning, showed that no measurable amount of new fines were generated. This means that fresh seed particles have to be conditioned and the generated fines must be removed before initiation of silane pyrolysis in a fluid bed.

4.2.3 High Frequency Capacitive Heating

The two objectives of the tests are that high-frequency electrical heating can be accomplished effectively in the 500 to 900°C range, and a favorable temperature gradient between the bed particles and the bed wall can be realized. To this end, the apparatus design

reported in the last quarterly progress report was redesigned to achieve improved temperature control and thermal measurements.

Recent silicon bed heating in the redesigned apparatus accomplished both objectives, i.e., the silicon bed was heated to 785°C and the bed particles were 12°C hotter than the bed wall. This temperature gradient between the bed and the wall is the key to minimizing silane pyrolysis on the reactor wall.

Figure 4.4 shows the test apparatus with the location of thermocouples labeled. Temperature distributions in steady-state, in two experiments, are shown in Tables 4.1 and 4.2. Table 4.1 shows test results from an experiment in which the outer guard heaters (Point E in Figure 4.4) are maintained only 10°-15°C colder than the bed wall, reducing the radial heat flux from the bed. In order to minimize the heat leak further, the lower flange (Point F) is also maintained at 15°C colder than the bed wall. Under these conditions heat leak from the bed is controlled to an estimated 70W. The feed gas is preheated by the flow of heat along the tube wall from Point F to Point D. The amount of preheating is accountable by measuring the gas temperature just before the gas enters the bed (Point A). The observed temperature gradients between the wall and the bed indicate a heat transfer coefficient of 200 $W/m^{2o}C$.

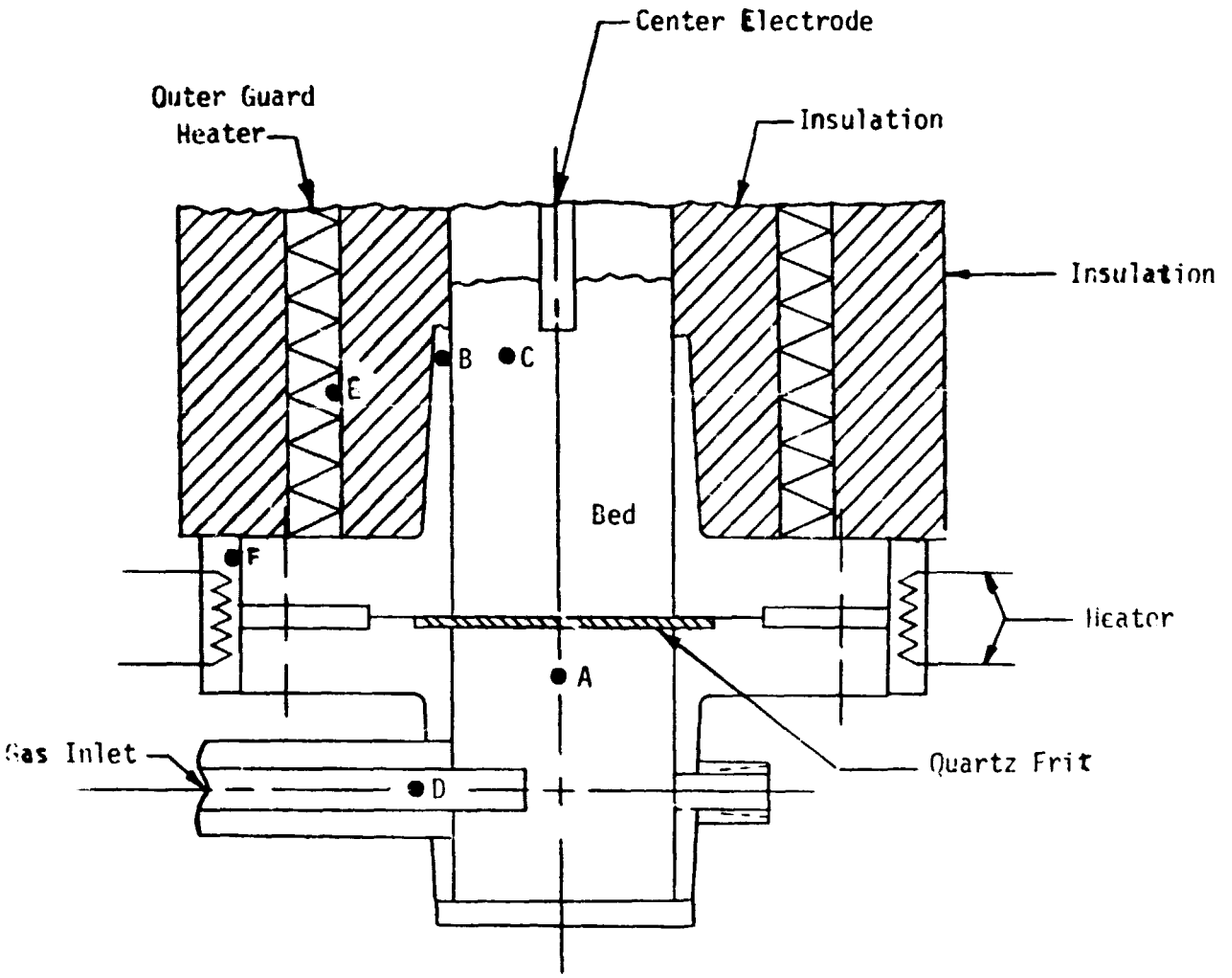

FIGURE 4.4 SCHEMATIC OF BED SHOWING POINTS OF TEMPERATURE MEASUREMENT

TABLE 4.1

TEMPERATURE DISTRIBUTIONS/RESULTS TEST 1

Electrical Dissipation in Bed	250 W
Electrical Frequency	75 k Hz
Voltage	44 V
Current	18 A
Phase Angle	45^{o}

Temperature Distribution

Point		T(^{o}C)
A	Gas Inlet to Bed	487
B	Bed Wall	772
C	Bed Particles	785
D	Gas Inlet to Apparatus	207
E	Guard Heater	760
F	Outer Flange	760

Heating results with guard heating preventing side heat loss. Note temperatures are maintained so there is still heat loss from bed, not heat addition.

TABLE 4.2

TEMPERATURE DISTRIBUTIONS/RESULTS TEST 2

Electrical Dissipation in Bed	200 W
Electrical Frequency	15 k Hz
Voltage	24 V
Current	18 A
Phase Angle	22^{o}

Temperature Distribution

Point		T(^{o}C)
A	Gas Inlet to Bed	210
B	Bed Wall	277
C	Bed Particles	301
D	Gas Inlet to Apparatus	184
E	Guard Heater	215
F	Outer Flange	240

Heating results without guard heating, hence high side heat loss.

The results given in Table 4.2 are for a similar experiment, except that the guard heating is absent, allowing large radial heat flux. This condition increases the bed particles-to-reactor wall temperature difference to $24^{o}C$, and reduces the attainable bed temperature to $301^{o}C$. By running experiments at higher power, higher wall-to-particle temperature differences can be maintained.

The electrical behavior of the bed is similar to that at low temperature. There is an initial transient state in which the bed impedence is high ($\sim 50\ \Omega$), after which it drops to $\sim 1\text{-}3\ \Omega$. This latter steady impedence is dependent on the position of the electrode, and can be raised by partially removing the electrode from the bed. The lower impedence also has a reactive component, corresponding to approximately $0.5\ \mu F$ of capacitance. Since the origin of the transition between states is unknown, the origin of this capacitance is also unknown. However, the electrical energy can be dissipated readily in the bed, and even when it is confined to only the upper portion of the bed, particle motion quickly distributes the heat evenly. On this basis, direct electrical heating can be used to maintain a fluidized bed at the temperature required for pyrolysis, with the walls substantially colder.

4.2.4 Boot Tests

A simple boot was attached to the bottom of the 6-inch glass column. The bed was operated at 1/6 atmosphere to simulate the gas mass density expected in the PDU. Qualitative differences in bed behavior were observed with and without the boot. A single large bubble seems to move up the center of the bed with the boot; while, with a flat distributor plate, small bubbles are dispersed across the bed. Even with the boot, however, there is a large stable bubbling range ($1 < U/U_{mf} < 3$) as evidenced by the velocity-pressure drop measurements.

In a preliminary test of particle segregation by size, a small amount of particles having twice the mean diameter of the average bed particles was added to the bed. After the run, size distributions in the bulk of the bed and in the boot were measured as shown in Figure 4.5. There appears to be a tendency for large particles to collect away from the boot. Further tests are required to learn more about the mechanics of particle segregation.

4.3 CONCLUSIONS

The following can be concluded from the test results in this quarter:

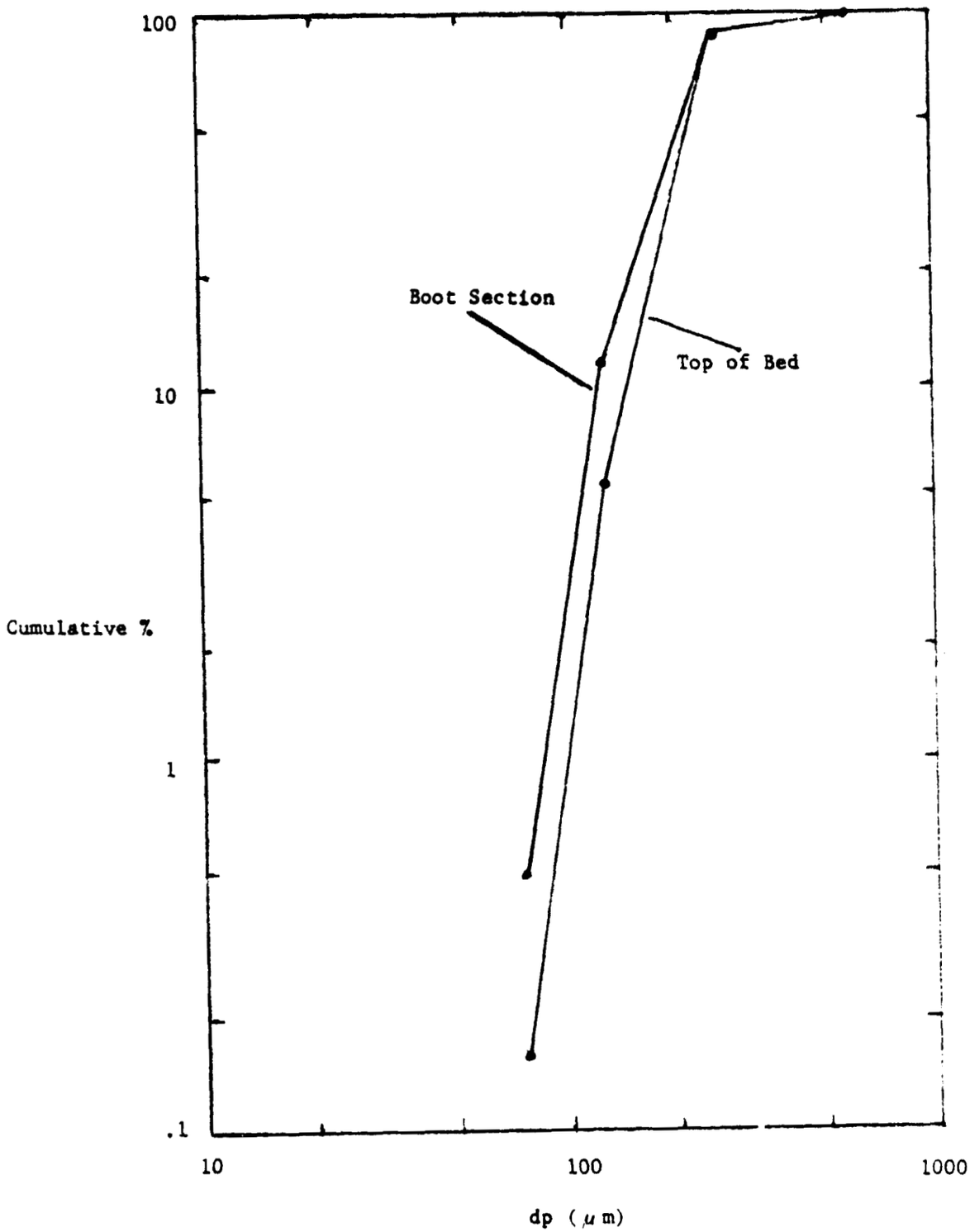

FIGURE 4.5 Cumulative weight distribution vs. mesh diameter of particles from boot section and from top of bed.

- A silicon bed can be operated stably at low gas densities. In other words, the effect of gas density on the bed behavior is not as strong as expected.
- The bed can be operated without slugging up to gas velocities twice the minimum fluidization velocity.
- For dense, coherent particles, the attrition rate is very slow.
- A silicon bed was heated by high-frequency capacitive heating to 785 °C, high enough for silane pyrolysis. The reactor wall temperature was 12°C below the bed temperature. This temperature gradient is desirable to maximize heterogeneous decomposition of silane on the bed particles.
- A silicon bed can be fluidized stably with a boot section at the bottom of the bed.

4.4 PROJECTED QUARTERLY ACTIVITIES

4.4.1 Technical Summary Report

A technical summary report will be prepared which will contain all detail work accomplished under this program.

4.4.2 Final Technical Report

Work performed under this program will be included in the overall Phase II final technical report to be issued on March 1, 1979.